Alma Mater Studiorum – Università di Bologna

DOTTORATO DI RICERCA IN

SCIENZE BIOMEDICHE

Ciclo XXVIII

Settore Concorsuale di afferenza: 06/A3

Settore Scientifico disciplinare: MED/07

TRANSFER OF VIRAL AND MITOCHONDRIAL NUCLEIC ACIDS THROUGH MICROVESICLES: A POSSIBLE MECHANISM OF GENETIC INTRA-TUMOR HETEROGENEITY IN BREAST CANCER

Presentata da: Dott.ssa Claudia Savini

Coordinatore Dottorato
Chiar.mo Prof. Lucio Cocco

Relatore:
Dott.ssa Monica Cricca

Tutor:
Chiar.ma Prof.ssa Maria Carla Re

Esame finale anno 2016

Introduction

Microvesicles

Microvesicles (MVs) are small extracellular vesicles physiologically secreted by cells in order to guarantee cell to cell communication. These MVs can be secreted by different cells, tissues and body compartments such as hematopoietic cells, dendritic cells, T and B lymphocytes, platelets, macrophages, mastocytes, epithelial cells, fibroblasts and so on. Microvesicles have also been widely detected in various biological fluids including peripheral blood, urine and ascitic fluids; their function and composition depend on the cell from which they originate (Graves LE, et al., 2004; Piccin A, et al., 2007; Smalley DM, et al., 2008; Taylor DD, and Gercel-Taylor C, 2008). Under stress conditions like hypoxia, radiations or oxidative stress, cells tend to secrete more MVs (Ratajczak J, et al., 2006).

Studies over the past few years have shown that microvesicles can contain bioactive molecules, nucleic acids and/or proteins (Cocucci E, et al., 2009), where microvesicles packaged with microRNAs (miRNAs) or mRNAs are mainly released from progenitors of differentiated cells and tumor cells (Ratajczak J, et al., 2006). Due to their heterogenic membrane, cargo, size, origin and function, there is not a precise categorization of the MVs thus, as of today, microvesicles are divided in 3 main groups according to their size (Meckes DG, et al., 2011):

1. Exosomes (40-100nm)
2. Shedding microvesicles (100nm –1μm)
3. Apoptotic bodies (1–5μm)

Exosomes

The first evidence of exosomes was in 1981 when Trams and colleagues reported that normal and neoplastic cell lines exfoliated shedding vesicles with sizes ranging from 40 to 100 nm and a circular morphology, under electron microscopy (Trams EG, et al, 1981).

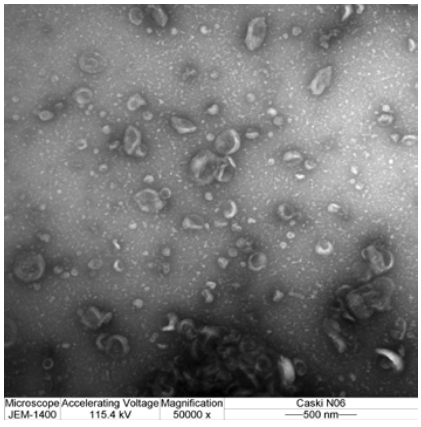

Figure 1: Electron microscopy on MVs coming from Caski cell line (HPV16 positive)

The endocytic pathway is a convoluted web of interconnected sub-compartments with distinct cell localization, pH, lipid and protein composition, in which cells internalize ligands by endocytosis concomitantly with membrane proteins and lipids. Exosomes are generated by inward budding of the lumen of internal vesicular compartments derived from endosomes (Thery A, et al., 1999). As vesicles accumulate within these endosome-derived compartments, they are referred to as multivesicular bodies (MVBs). The internalized material can be sent for degradation through maturation into MVBs and fuse together with lysosomes (Bainton D.F., 1981). Alternatively, cargo can be re-routed for recycling or secretion. Recycling processes are categorized into a quicker and a slower pathway depending on the time that proteins and lipids take from internalization to exposure back at the cell surface (or release to the extracellular media in case of luminal soluble factors) (Mobius W, et al., 2003). Secretion of exosomes requires maturation of early endosomes into MVBs, with concomitant formation of intraluminal vesicles (ILVs), and fusion of MVBs with the cell surface to release exosomes. ILVs formation is characterized by inward budding of membranes, a process that starts in early endosomes but greatly augments as endosomes mature. At any point material can be further internalized to the trans-Golgi network and integrated in canonical secretory pathways (Scott CC, et al., 2014).

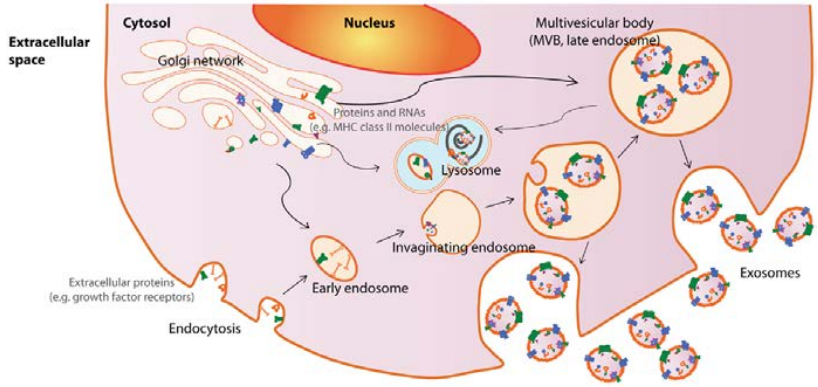

Figure 2: Exosome biogenesis and secretion (Zhang B. et al., 2014)

The exosomes released in the extracellular environment can be transferred to near or distant cells. The mechanism by which this occurs is not entirely clear yet but the hypotheses are: 1) ligand receptor interaction, 2) lipid membrane fusion and 3) endocytic entry of the exosomes in the recipient cell.

Proteomic analysis of the exosomes' cargo showed that these MVs contain different types of proteins and lipids, mostly coming from the plasma membrane, the cytosol, the nucleus or the endoplasmic reticulum of the donor cell.

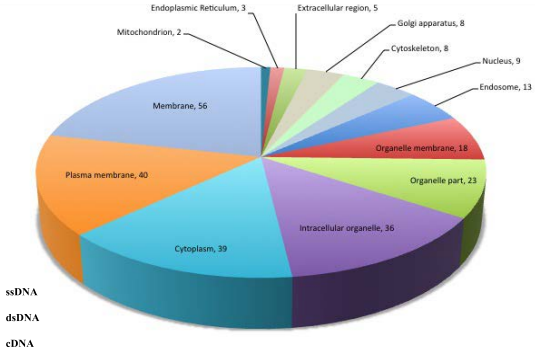

Figure 3: Molecular composition of exosomes (Rappa G, et al., 2013)

Shedding Microvesicles

Shedding microvesicles derive from the plasma membrane and have a size between 100 nm to 1 µm.
Similar to the exosomes, these MVs contain RNA and microRNA, have a lipid composition and are secreted under physiological and stress conditions. These vesicles can also contain integrins, cytokines, chemokines, metalloproteases and high levels of phosphatidylserine (Meckes DG, et al., 2011).

Apoptotic Bodies

Cells undergoing apoptosis partially transform into phosphatidylserine-containing apoptotic bodies, which are rapidly engulfed by phagocytes or neighboring cells to inhibit an inflammatory response or prevent the unwanted activation of the coagulation system. These microvesicles are covered by a lipid membrane and characterized by a large size ranging from 1 to 5 µm.
Once released, these vesicles can internalize cellular organelles and DNA fragments like oncogenes. Since their isolation is more complicated compared to the isolation of exosomes, little is known about their composition, cargo and function; despite knowing that they play an important role in the antigen presentation during immunosuppression (Meckes DG, et al., 2011).

Microvesicles and tumor microenvironment

Although a microvesicle shedding occurs under physiological conditions, aberrant release of microvesicles can arise in disease states. Many studies demonstrated that the tumor microenvironment is rich of microvesicles secreted by tumor cells, lymphocytes and monocytes, which are located in the tumor tissues. These MVs stimulate the production and secretion of several pro-angiogenic factors by the stromal cells, leading to cell proliferation, angiogenesis and cellular invasiveness.
Other than *in vitro* evidence of a higher production of microvesicles from the tumor cells, patients affected by cancer show a higher number of circulating MVs in the bloodstream and this correlates with a worse prognosis of the illness (Rak J, 2010). Microvesicles in cancer patients were first documented in 1978, when they were identified in cultures of spleen nodules and lymph nodes of a male patient with Hodgkin disease (Friend C, et al., 1978).
Microvesicles shed from tumor cells facilitate transfer of soluble proteins (Iero M, et al., 2008), nucleic acids (Skog J, et al., 2008), functional trans-membrane proteins, tissue factors (Del Conde I, et al., 2005), chemokine receptors (Mack M. et al., 2000), and receptor tyrosine kinases such as epidermal growth factor receptor (EGFR) and human epidermal growth factor receptor 2 (HER2) (Al-Nedawi K, et al., 2008; Sanderson MP, et al., 2008). Different studies showed that the presence of specific proteins in the microvesicles is correlated with tumor growth.

Table 1 summarizes the most important ones.

Protein type	Proteins of interest	Functional significance	References
Soluble	Proteases (MMP2, MMP9, uPA)	ECM degradation upon rupture of released microvesicles	(Angelucci et al., 2000; Ginestra et al., 1998; Baj-Krzyworzeka et al., 2006; Sidhu et al., 2004)
	VEGF	Promotes angiogenesis	(Baj-Krzyworzeka et al., 2006; Taraboletti et al., 2006; Kim et al., 2002)
Membrane associated	β1 integrin	ECM attachment	(Dolo et al., 1998; Muralidharan-Chari et al., 2009)
	Proteases (MT1MMP, Cathepsin B)	ECM modification and MMP activation	(Hakulinen et al., 2008; Giusti et al., 2008; Taraboletti et al., 2006; Dolo et al., 1998)
	MHC-class I	Not defined. Antigen presentation?	(Dolo et al., 1998; Muralidharan-Chari et al., 2009; Baj-Krzyworzeka et al., 2006)
	EGFR	Receptor tyrosine kinase signal transfer	(Al-Nedawi et al., 2008)
	VAMP3	v-SNARE	(Muralidharan-Chari et al., 2009)
	ARF6	Regulation of microvesicle release	(Muralidharan-Chari et al., 2009)
	HER2	Receptor signal transfer	(Sanderson et al., 2008)
	TNFL6 (FasL)	Immune evasion, promotes T-cell apoptosis	(Andreola et al., 2002; Huber et al., 2005; Kim et al., 2005)
	LMP-1	Immune evasion; inhibits leukocyte proliferation	(Flanagan et al., 2003)
	CD147/EMMPRIN	Proangiogenic activity and ECM degradation either directly or by activation od cancer stem cells	(Millimaggi et al., 2007; Baj-Krzyworzeka et al., 2006; Sidhu et al., 2004)
	Tissue Factor	Thrombus formation, activation of cancer stem cells	(Zwicker et al., 2009; Milsom et al., 2007)
	MUC1	Not defined. Facilitates thrombus formation by increasing plasma viscosity?	(Tesselaar et al., 2007)
Cytoskeleton associated	Actin	Not defined. Cortical microvesicle skeleton?	(Charras et al., 2005; Paluch et al., 2005; Muralidharan-Chari et al., 2009)
	Myosin	Pinching of vesicle neck during release of microvesicles	(McConnell et al., 2009; Muralidharan-Chari et al., 2009)

Table 1: Tumor-derived microvesicles and their potential role in cancer progression (Muralidharan-Chari V, et al., 2009)

Cancer cells interact with the stroma and actively modify the microenvironment to favor their own progression (Fidler IJ, et al., 2008). A recent study showed a mechanism of reciprocal communication between cancer cells and microvesides: MVs released by PC3 cells, an invasive prostate cancer cell line, increased motility and resistance to apoptosis in fibroblasts in the surrounding microenvironment. In turn, the activated fibroblasts shed microvesicles to facilitate the migration and invasion of the prostate cancer cell line (Castellana D, et al., 2009). Similarly, Di Vizio and colleagues confirmed the role of prostate-tumor-derived microvesicles in the 'activation' of stromal cells in the tumor microenvironment (Di Vizio D, et al., 2009).

Matrix degradation is essential for promoting tumor growth and metastasis (Hotary K, et al., 2006). As indicated above, microvesicles that are shed by tumor cells are loaded with proteases and provide additional means of matrix degradation, creating a path of least resistance for invading tumor cells. Given the importance of matrix degradation in tumor metastases, it is logical to hypothesize that there is a direct correlation between the number of invasive microvesicles and tumor progression.

Microvesicles cargo: viral and mitochondrial components

Viral components were found in cells in which viral entry should be avoided due to the absence of specific receptors on their surface (eg. HPV, HIV). This discovery led to the hypothesis that microvesicles could act as mechanism of exit, transfer and entry from a permissive host cell to another.
The viral contents of exosomes, until now, was investigated for HIV, hepatitis C virus (HCV), HBV, human T-lymphotropic virus (HTLV), Human Papillomavirus (HPV) and Epstein Bar Virus (EBV).
In 2000, Mack and colleagues (Mack M, et al., 2000) demonstrated the transfer of the viral HIV CCR5 receptor (needed for the virus entry in the host cell), from CCR5 positive cells to CCR5 negative cells through microvesicles; this result led to the hypothesis that HIV could use these vehicles to infect cells lacking its receptor and help its spread into the host. In 2013, exosomes from HCV-infected cells were shown to be capable of transmitting infection to naïve human hepatoma cells and establishing a productive infection. This discovery led to the conclusion that viruses could actually use microvesicles to escape the immune system (Ramakrishnaiah V, et al., 2013).
Additionally, microvesicles from lymphoblastoma cells have shown to expose the EBV latent membrane protein (LMP-1), another immune-suppressing trans-membrane protein, which inhibited leukocyte proliferation (Flanagan J. et al., 2003). Since many viruses, in the absence of a full blown primary infection (CMV, SV40, HHV8 and HSV1, HPV, EBV), were found in tumor tissues (Hermann K, and Niedobitek G, 2003; Doorbar J, 2015), as well as in sites which are not permissive to viral entry, microvesicles can be considered as a possible mechanism of transfer of viral material from a tissue to another.

Other than viral components, microvesicles can also transfer mitochondria. In particular, a study conducted in 2013, showed the release of large microvesicles (1 to 8 μm) from human fetal astrocytes in culture, containing mitochondria. They were also able to demonstrate that the mitochondria in the vesicles were active and functional (Falchi AM, et al., 2013).

Oncogenic Viruses

Oncogenic viruses are viruses able to induce tumors in their natural host or in animal models. The first evidence that tumors could be caused by viruses was in 1908 when Francis Pyton Rous found that the avian sarcoma could be transmitted from host to host without the transfer of a cellular component. This discovery led to the idea that particles smaller than cells could be the cause of such pathology (Rous P, 1911).
After this fundamental discovery many other different viruses linked to cancer development were discovered, like the Human Papillomavirus (HPV) and the Epstein Barr Virus (EBV). The possibility that cervical cancer could be a sexually transmitted pathology was known since 1800. This is why Haral zur Hausen thought that HPV, known to cause genital warts, could be responsible for this neoplasia (zur Hausen H, 1976). He was able to identify high risk HPV DNA sequences (HPV16 and HPV18), which were later found to be the most frequent in cervical cancers (zur Hausen H, 1983; Boshart M, et al. 1984). Earlier in 1964 the first human oncovirus was described by Anthony Epstein, Bert Achong and Yvonne Barr who, thanks to electron microscopy experiments were able to identify EBV in African patients affected by Burkitt' s lymphoma (Epstein MA, et al., 1964).
The mechanism by which oncoviruses are able to lead to cellular transformation is mediated by the insertion or the expression of viral sequences in the host genome, which alter the cellular physiology leading to a higher expression of cellular proto-oncogenes or viral proteins production (zur Hausen H, 1999).
Human oncoviruses are not usually found as viral particles, since they tend to be found in a latent form where the viral nucleic acids persist in a plasmidic or episomal form that take advantage of the replicative machinery of the host cell in order to divide (zur Hausen H, 2009).

Human Papillomavirus

Classification

Human Papillomaviruses belong to the *Papillomaviridae* family that contains more than 120 different HPV genotypes divided in two groups, called mucosal or epithelial, depending on the site of infection (de Villiers EM, et al., 2004). HPV can be transmitted either sexually or by direct contact with an infected sharpened surface that determines the formation of epithelial lesions. Some HPVs preferentially infect the epithelial cells of the anogenital tract and can be divided in low and high risk depending on their oncogenic potential (de Villiers EM, et al., 2004). While the low risk HPVs lead to the formation of genital warts, a benign cellular proliferation, the high risk HPVs (eg. HPV16 and HPV18) are responsible of the cervical cancer where HPV16 has been consider the most oncogenic HPV subtype, by the Internation Agency for Research on Cancer (IARC). In particular, HPV16 was identified in the 60% of the high grade intraepithelial cervical dysplasia, in the 50% of the anogenital cancers and somehow in the oral, pharyngeal and lung cancers; HPV18, otherwise, is mostly associated to adenocarcinomas.

Genome organization

Human papillomaviruses are small viruses with double stranded DNA (dsDNA) enclosed in an icosahedral capsid with 72 capsomers, of 52-55 nm. The viral genome has a length of about 8 Kbps which can be divided in 3 major regions called early (E), late (L) and long control region (LCR); the early region encodes for the early oncogenic proteins, the late region encodes for the capsid proteins while the LCR is a non coding region containing the origin of replication and the transcriptional factor binding region

The figure schematizes the genomic structure of HPV (Kajitani N, et al., 2012):

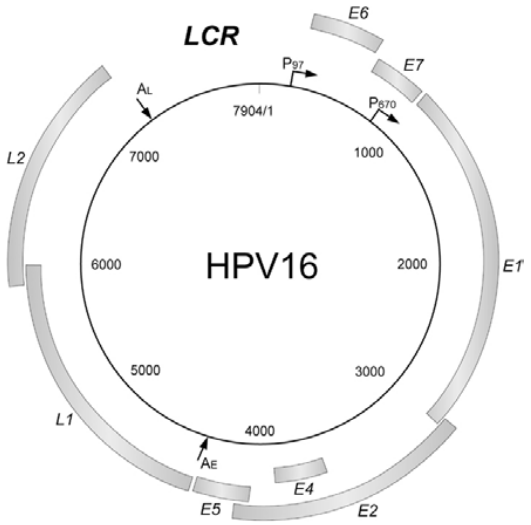

Figure 4: Genomic structure of HPV16 (Kajitani N, et al., 2012)

The proteins encoded by the HPVs are 7 and are called E1, E2, E4, E5, E6, E7, L1 and L2. Their functions are summarized in table 2:

Protein	Function
E1	Viral DNA replication
E2	Viral DNA replication; repression of E6/E7 genes
E4	Assembly and release of the viral particle
E5	Interaction with the Epidermal Growth Factor (EGF)
E6	Destruction of p53 tumor suppressor protein
E7	Inactivation of pRb tumor suppressor protein
L1	Major capsid protein in the viral particle
L2	Minor capsid protein in the viral particle

Table 2: Protein function of Human Papillomaviruses

Interacting with p53 protein, E6 impedes it to bind DNA in an effective way, and the p21 protein is therefore not available to act as the 'stop signal' for cell division. Thus cells divide uncontrollably, and form tumors. Additionally E7 binds to pRb, which cannot longer bind the E2F protein leading to cell proliferation, missing the G1-S cellular checkpoint. This causes the division of cells with possible mutation, thus the tumor progression (Giacinti C, 2006).

HPV life cycle and host transformation

HPV life cycle is strictly dependent on the differentiation status of its host cell, the keratinocyte, and a number of cellular proteins (Stubenrauch F, Lamins LA, 1999). The HPV infection starts in the stem cells of the basal layer, when the virus enters the cells through epithelial micro lesions. Once in the cell, the viral DNA goes to the nucleus as an extra chromosomal element and its early promoter is activated leading to the production of the E1 and E2 proteins that start the viral DNA replication producing 50 to 100 episomal copies. The number of DNA copies is then kept stable and their replication is linked to the cellular one. When the host cells divide, one differentiates while the other one remains stem functioning as a latent viral DNA reservoir. During cell differentiation, instead, the late promoter is activated and starts the productive phase of the viral life cycle that implicates the production of the late proteins L1 and L2 and the capsid assembly.

Since the presence of episomal HPV was only found in benign lesions, while integrated sequences of viral DNA were found in tumor tissues, this integration step has been considered fundamental for the host cell transformation process (Schneider-Maunoury S, et al., 1987). The integration site of HPV in the host genome appears random even if it is often found near specific loci like *c-myc* and *N-myc*, which are known to be fragile sites and, in high grade lesions, usually involves the E1 and E2 ORF of the viral DNA. In fact, the E1 and E2 breakage leads to an uncontrolled synthesis of E6 and E7 proteins with an abnormal cell proliferation as consequence. The integration site of HPV-18 in the human genome has been completely mapped in HeLa cells by Andrew Adey in 2013 (Adey A, et al., 2013). Adey found out that in chromosome 8q24.21 the integration of the HPV-18 genome occurred, which is likely to be the event that initiated tumorigenesis.

Epstein Barr Virus (EBV)

Classification

Herpesviruses are divided into three groups: α-herpesviruses, β-herpesviruses and γ-herpesviruses, where the Epstein-Barr is classified. They replicate in lymphoblastoid cells *in vitro* and can cause lytic infections in certain targeted cells. Latent viruses were demonstrated in lymphoid tissues. In particular, Epstein Barr virus replicates in the epithelial cells of the oropharynx and in β-lymphocytes and is transmitted by intimate contact, particularly via the exchange of saliva.

Genome Organization

The EBV genome consists of a linear dsDNA of approximately 172 Kbps coated by the capsid proteins and surrounded by a tegument layer which is enclosed by an envelope composed of bilayer proteins sandwiched by lipids (Odumade OA, et al., 2011). EBV has a series of internal repeat sequences (IRs) that divide the genome into short and long, largely unique sequence domains and 0.5 kb terminal direct repeats (TRs), responsible of the circularization of the viral DNA after infection. The virus has the coding potential for around 85 proteins, not all of which have been identified or characterized. During latency only a few viral genes are expressed and the viral genome persists as a multi copy circular episome. The episome contains repetitive sequences that serve as multiple cooperative binding sites for the viral DNA binding proteins Epstein Barr virus Nuclear Antigen 1 (EBNA1).

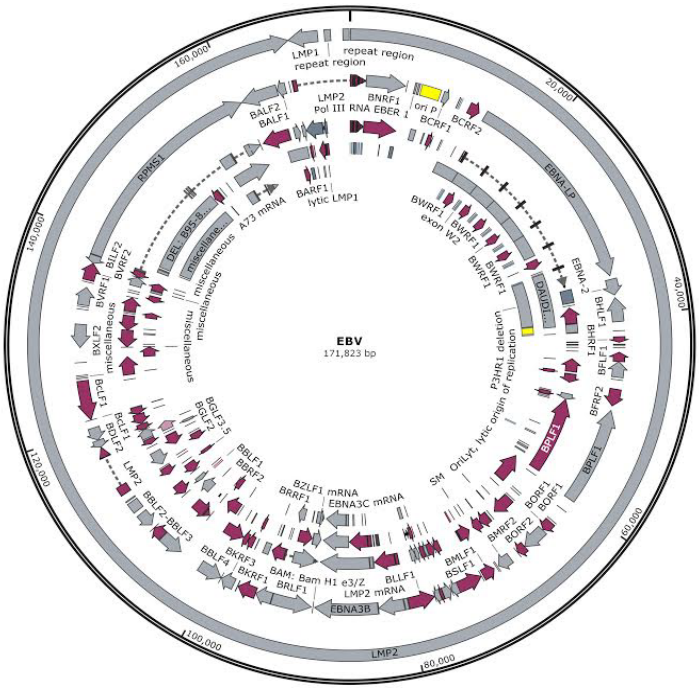

Figure 5: Epstein Barr Virus circular dsDNA (SnapGeneViewer Software)

EBV Life Cycle and host transformation

Transcription, genome replication, and capsid assembly occur in the host cell nucleus. Genes are replicated in a specific order: 1) immediate-early genes, which encode regulatory proteins; 2) early genes, which encode enzymes for viral DNA replication; and 3) late genes, which encode structural proteins. The tegument and envelope are acquired as the virion buds out through the nuclear membrane or endoplasmic reticulum. Virions are transported to the cell membrane and the host cell dies as mature virions are released. Alternatively, in selected cell types, the virus may be maintained in a latent state. The latent viral genome may reactivate at any time even though the mechanism of reactivation is not known.

The cascade of events in the lytic phase of the EBV life cycle is divided into three phases of regulated gene expression: immediate–early, early and late. The immediate–early gene products are trans-activator proteins that trigger the expression of the early genes, the products of which include enzymes that are required for viral DNA replication. In turn, amplification of EBV DNA defines the boundary between early and late gene expression. During the late phase of the cycle viral structural proteins are expressed and assembled into virus particles into which the DNA is packaged prior to release of infectious virions.

Studies on EBV have been facilitated since 1984, when Rickinson and colleagues, found that EBV could be cultured *in vitro* by using peripheral blood lymphocytes from healthy EBV sero-positive patients (Rickinson AB, et al., 1984); these cells give rise to spontaneous outgrowth of EBV-transformed, immortalized cell lines which are known as lymphoblastic cell lines (LCLs). Every cell now carries multiples copies of circular extra-chromosomal viral DNA, which circularizes by homologous recombination of the TRs, and produces a number of latent proteins like 6 nuclear antigens (EBNA 1, 2, 3, 3A, 3B, 3C and LP) and 3 latent membrane proteins (LMP 1, 2A and 2B).

EBV is associated with the development of both lymphoid and epithelial tumors. Its role in oncogenesis has been confirmed by its frequent detection in certain tumors like the Burkitt' s lymphoma (BL), the post-transplant B cell lymphomas, the Hodgkin's disease (HD), the nasopharyngeal carcinoma (NPC) and gastric cancer. *In vitro* experiments also showed the capacity of EBV to transform resting B cells and induce tumors in non-human primates (Henle G, et al., 1976; Pope JH, et al., 1968; Miller G, 1974). All tumors are characterized by the presence of multiple extrachromosomal copies of the circular viral genome and expression of the EBV-encoded latent genes, which appear to contribute to the malignant phenotype (Young LS, et al., 2004).

Early in the course of primary infection, EBV infects B-lymphocytes, establishing a latent infection, characterized by the limited expression of a subset of viral latent genes and small non-coding RNAs, like EBERs 1 and 2. Many studies focused on the importance of the latent proteins in oncogenesis, leading to the discovery that EBNA1 is required for the maintenance of the episomal EBV genome (Young LS, et al., 2004), while EBNA2 is responsible for the activation of LMP1, the major EBV transforming protein. In particular, LMP1 acts up regulating antiapoptotic cellular proteins (Henderson S, et al., 1991; Laherty CD, et al., 1992), and stimulating the production of cytokines (IL-6, IL-8) (Eliopoulos AG, et al., 1997; Eliopoulos AG, et al., 1999). LMP1 was reported as the major oncogenic factor of nasopharyngeal carcinoma (NPC) development and was detected in 80-90% of NPC tumors (Pioche-Durieu C, et al., 2005). In addition to the latent proteins, EBERs 1 and 2 are involved in EBV mediated pathogenesis, since their presence is correlated with the production of the IL-10 cytokine.

The most known latent genes, their proteins and functions are summarized in figure 6:

GENE	GENE PRODUCT	POSTULATED FUNCTION
BKRF1	EBNA-1	viral genome maintenance essential for *in vitro* immortalization of B cells
BYRF1	EBNA-2	viral oncogene essential for *in vitro* B-cells immortalization
BLF3-BERF1	EBNA-3A	essential for in vitro B-cell immortalization
BERF2α-BERF2β	EBNA-3B	not known
BERF3-BERF4	EBNA-3C	viral oncogene essential for in vitro B-cell immortalization
BWRF1	EBNA-LP	not known
BNLF1	LMP-1	induces lymphoblastoid phenotype tumor necrosis factor receptor superfamily member
BARF1/BNRF1	LMP-2A	prevents cell activation and lytic-cycle entry
BNRF1	LMP-2B	not known
BCRF1	EBER1, EBER2	regulates PKC activity upregulates *bcl2* on Burkitt's lymphoma cells
BARF0	BamHIA transcripts	not known

Figure 6: EBV principal viral latent genes (Leone G, et al., 2009)

Mitochondrial DNA heterogeneity in cancer

Mitochondria are indispensable organelles found in the cellular cytoplasm that orchestrate several homeostatic functions of the cell. The primary function of mitochondria is to generate large quantities of energy in the form of ATP; they also store calcium for cell signaling activities, generate heat and mediate cell growth and death. Since mitochondria are independent organelles evolving from a bacterial progenitor via symbiosis within an essentially eukaryotic host cell, they have their own DNA. The mitochondrial genome (mtDNA) is a closed dsDNA molecule of about 16.6 Kbs composed of a heavy (H) strand and a light (L) strand. Most of the information is encoded on the heavy strand but the 13 protein products encoded by both the heavy (12 polypeptides) and light (1 polypeptide) strands are constituents of the enzyme complex of the oxidative phosphorylation system (Anderson S, et al., 1981; Macreadie IG, et al., 1983; Chomyn A, et al., 1985).

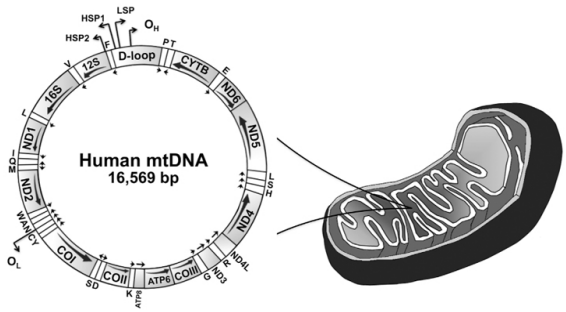

Figure 7: Replicating animal mitochondrial DNA (Emily A, et al., 2013)

Even if the mitochondrial DNA is extremely small compared to the genomic one and constitutes about the ~1% of the total cellular DNA, like the genomic DNA, can sustain mutations which can randomly or selectively increase in affected tissues. Several repeats in the mtDNA serve as breakpoints that characterize large-scale deletions, where the major one is comprised between the CytB – COI region and flanked by the light and heavy origins of replication. Other rare rearrangements are reported, including inversions, simple insertions of small bases of up to 300 and complex rearrangements with kb inserts. This condition in which mutant and wild type mtDNA coexist is called *heteroplasmy* ad is a known hallmark of mitochondrial disease. Other than changes in the mitochondrial genome, changes in its number can occur and this state is linked to certain pathologic conditions and cancers. Mitochondrial DNA copy number refers to the number of functional genomes per cell or tissue. Copy number changes are important in cancer since they can modulate cancer initiation, cause nuclear genome instability, and therapy response. According to a study performed by Brandon and colleagues (Brandon M, et al., 2006), there are two distinct types of mtDNA mutations in cancer: 1) pathogenic (possibly carcinogenic), in which the probability to compromise the mitochondrial bioenergetics - leading to the increased production of ROS - is high; and 2) adaptive mutations, which enable cancer cells to adapt to new microenvironments.
Since a transfer of nucleic acids between cells through microvesicles was established and demonstrated, it is not absurd to hypothesize a possible mechanism of transformation or tumor progression by the transfer of mutated mtDNA from already transformed cells to the surrounding wild type ones.

Microvesicles as a tool of nucleic acids transfer

The presence of ssDNA, cDNA (Balaj L, et al., 2011), dsDNA (Thakur BK, et al., 2014), RNA (Skog J, et al., 2008) and miRNA (Chen X, et al., 2008; Lawrie CH, et al., 2008; Mitchell PS, et al., 2008), in the microvesicles has been demonstrated. In particular, MVs coming from tumor cells *in vitro* and *in vivo* showed an amplification of the *c-Myc* oncogene as well as retrotransposon RNA elements together with a higher amount of nucleic acid content compared to the MVs coming from healthy donors or normal fibroblasts (Balaj L, et al., 2011).
In 2010 Pegtel et al., thanks to co-colture experiments, demonstrated the secretion of exosomes containing functional viral miRNAs by lymphocytes B infected by EBV (Pegtel DM, et al., 2010). A study conducted in 2012 characterized the presence of viral DNA in apoptotic bodies coming from HPV positive cells and its transfer to primary fibroblasts; interestingly, the recipient fibroblasts showed the typical signs of transformation suggesting that the viral content was functional (Gaiffe E, et al., 2012). A part from that, little is known about the viral nucleic acids content in the microvesicles.
Other than viral nucleic acids, exosomes were shown to transfer mitochondrial DNA (Guescini M, et al., 2010), leading to the hypothesis that the nucleic acid material transferred from the MVs to the recipient cells, could be imported into mitochondria.
The discoveries that the MVs content could be transferred and change the recipient cells phenotype, led to the hypothesis that those MVs could have a role in cancer progression and heterogeneity. In fact, many studies described the presence of foreign material (viral nucleic acids or mutated mitochondrial DNA) in cancer tissues compared to normal tissues. Microvesicles coming from infected cells or mutated cells could transfer their material to recipient cells altering their phenotype and contributing to their transformation.
Until now, however, there have been no studies that explored the presence of other complex nucleic acid structures called R-loops, which are known to form during natural processes such as replication or transcription, but are also known to cause genome instability.

R-loops

R-loops were first described in 1976 when their formation *in vitro* was visualized by electron microscopy (Thomas M, et al., 1976). In 1994, Drolet and colleagues (Drolet M, et al., 1994), showed the formation of R-loops in live bacteria for the first time. Since then, many studies were conducted to understand the biogenesis and role of these particular structures. Recent genome-wide approaches permitted the detection of R-loops in many *loci* identifying a high number of putative R-loop-forming sequences (250,000) in 59% of human genes (Wongsurawat T, et al., 2012).

R-loops are structures in which an RNA strand is base paired to the template DNA strand and the non template DNA strand remains single stranded. These structures are found both in prokaryotic and eukaryotic organisms and are a consequence of transcription processes. Transcription and high G density zones are necessary for their formation (Daniels GA, et al., 1995; Zarrin AA, et al., 2004). Ginno and colleagues recently demonstrated that transcription through regions of GC skew leads to the formation of long R-loop structures (Ginno PA, et al., 2012) while Helmrich et al., suggested the possibility that the R-loops form at common fragile sites (Helmrich A, et al., 2011).

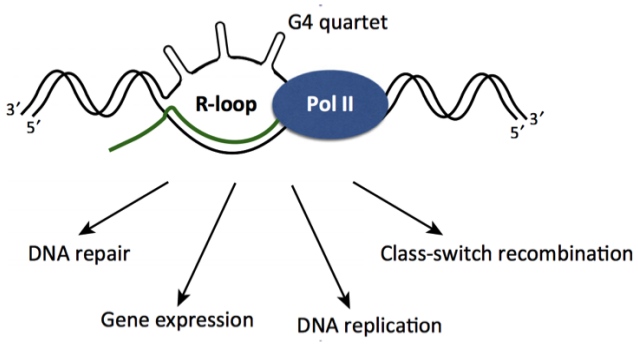

Figure 8: Physiological roles of R-loops in cells (Sollier J, and Cimprich KA, 2015)

Mainly, R-loops are known to be necessary during mitochondrial DNA replication (Xu B, and Clayton DA, 1996) and immunoglobulin class switch recombination (Yu K, et al., 2003). Other than that, R-loops have were also found to participate in epigenetic mechanism like DNA methylation and post-translational histone modification (Ginno PA, et al, 2012; Nakama M, et al., 2012; Castellano-Pozo M, et al. 2013; Yang Y, et al. 2014). However side effects were discovered; R loops, in fact, can also be dangerous sources of DNA damage, sensitizing DNA to damaging agents (Santos-Pereira JM, et al. 2013), inducing transcription associated recombination (Huertas P, Aguilera A, 2003), or double-strand breaks (Sordet O, et al. 2009). In particular, a study conducted by Bhatia and colleagues (Bhatia V, et al., 2014), correlated an increased formation of R-loops structures in HeLa cells lacking the BRCA2 protein, a double-strand break repair factor. They were also able to verify that the formation of R-loops is also correlated with transcription processes since, slowing or blocking the transcription fork, leads to the formation of DNA:RNA hybrids.

Breast cancer

Breast cancer is the most common cancer in women worldwide, with nearly 1.7 million new cases diagnosed in 2012 (second most common cancer overall after lung cancer). This represents about 12% of all new cancer cases and 25% of all cancers in women (World Cancer Research Foundation, http://www.wcrf.org/). Breast cancer is a hormone related illness and the factors that modify the risk of this cancer, when diagnosed pre-menopausally or post-menopausally, is not the same. It was demonstrated that a third of the breast cancers is related and supported by estrogens (Bajetta E, et al., 2000). Mammary cells have specific hormone receptors, particularly for progesterone and estrogen and it seems that estrogens are responsible for the induction of cell proliferation (Rana A, et al., 2010).

Breast cancer is an epithelial tumor deriving from an unchecked proliferation of the ductal and lobular cells in the mammary gland. It can be separated into different types based on the way the cancer cells look under the microscope. Mostly, breast cancer is a *carcinoma*, a type of cancer that starts in the epithelial cells, or *adenocarcinoma*, which starts in the glandular tissue. Breast cancers can be divided in invasive and not invasive cancer. In the first category we can find the ductal carcinoma *in situ* (DCIS or intraductal carcinoma), in which the cells that lined the ducts changed to look like cancer cells but do not spread through the walls of the ducts into the surrounding breast tissue. In the invasive breast cancer category we can find two main types of breast cancers, the invasive ductal carcinoma (IDC) and invasive lobular carcinoma (ILC). The first one is the most common type of breast cancer. It starts in a milk duct of the breast and, after breaking through the wall of the duct, grows into the fatty tissue of the breast. Here it can metastasize to other parts of the body through the lymphatic system and bloodstream. The second one, instead, starts in the milk-producing glands (lobules) and, like the IDC, can metastasize.

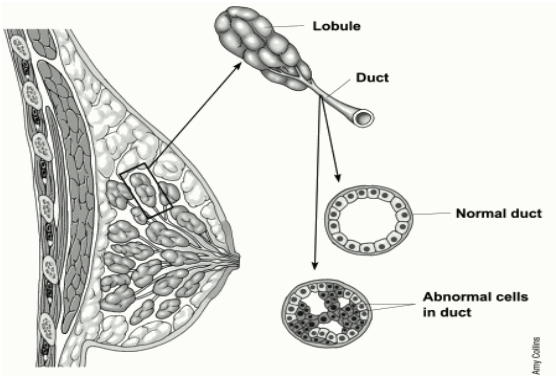

Figure 9: Ductal Carcinoma in Situ (DCIS) (www.cancer.org)

The main difference between each type of breast cancer is the expression of specific genes of the luminal epithelial cells, like the estrogen receptor (ER) and the progesterone receptor (PR).

Normal breast cells and some breast cancer cells contain receptors that attach to estrogen and progesterone. These two hormones often fuel the growth of breast cancer cells. Cancer cells may lack, one, or both of these receptors. Breast cancers that have estrogen receptors are often referred to as *ER-positive* (or ER+) cancers, while those containing progesterone receptors only are called *PR-positive* (or PR+) cancers.

Considering the hormone receptors and HER-2 status, breast cancers can be classified in 6 main categories:

1. Hormone receptor-positive: breast cancers which are either estrogen or progesterone receptor positive; can be treated with hormone therapy drugs that target the receptors lowering their number or blocking them. Women with these cancers tend to have a better prognosis even if it's not rare that the tumor comes back many years after treatment.
2. Hormone receptor-negative: breast cancers without any of the hormone receptors. Treatment with hormone therapy drugs is not helpful and it's for this reason that these types of tumors tend to grow more quickly than the hormone receptor-positive cancers.
3. HER-2 positive: cancers that express or amplify too much HER-2. These cancers can be targeted with HER-2 targeting drugs.
4. HER-2 negative: these cancers don't show an excess of HER2 and thus don't respond to HER2 targeting drugs.
5. Triple-negative: cancers that don't have estrogen or progesterone receptors and too much HER2. These cancers tend to grow and spread more quickly than all the other types of breast cancer because no drugs can be used against them.
6. Triple-positive: estrogen and progesterone receptor positive cancers; they show a high expression of HER-2. These cancers can be treated with hormone receptor drugs and HER2 targeting drugs.

Thanks to the microarray assay, 4 different types of breast cancer were discovered (Sørlie T, 2004):

1. Luminal A and Luminal B types: these types of breast cancer are ER+. The gene expression pattern of these cancers is similar to normal cells that line the breast ducts and glands. The Luminal A types are low grade cancers which tend to grow slowly and show the best prognosis.
2. The Luminal B cancers grow faster than the A ones, thus the prognosis is worse.
3. HER2 type: cancers characterized by having extra copies of the HER-2 gene and a high-grade appearance under the microscope. They tend to grow quickly and to have a worse prognosis although they can be treated with HER-2 targeting drugs and chemotherapy.
4. Basal type: these types of cancer are usually called triple negative due to the absence of the estrogen and progesterone receptors and a low expression of HER2.

HPV and EBV in breast cancer

Different studies correlated the insurgence of breast cancer to some viral infections like Simian Virus 40 (SV40), Cytomegalovirus (CMV) (Taher C, et al., 2013) and Epstein Barr virus (EBV) (Bonnet M, et al., 1999).

In 1992 Di Leonardo discovered the presence of HPV16 DNA sequences in the 29.4% of breast cancer tissues and some metastatic lymph nodes (Di Leonardo A, et al., 1992). After this discovery many other research groups detected HPV DNA sequences in breast cancers worldwide. The prevalence of HPV positive breast cancer is reported to vary from the 4% in Mexican to the 86% in American women (Heng B, et al., 2009). In 2012 Simões conducted a meta-analysis study estimating a global prevalence of HPV in breast cancers of about the 23% (Simões PW, et al., 2012). In 2004 the presence of HPV DNA sequences in breast cancer patients with a cervical pathology was discovered (Widschwendter A, et al., 2004), opening the possibility that the HPV viral nucleic acids could be transferred from a primary site of infection to a secondary not usual tissue.

Other than in the breast cancer tissues, HPV sequences were also found in other extragenital lesions like lung tumors (Chen YC, et al., 2004), head and neck carcinomas (zur Hausen H, 2009) and glioblastomas (Vidone M, et al., 2014).

The first evidence of the presence of EBV DNA in breast cancer tissues dates back to 1995 when Labracque et al., looked for the presence of this virus in almost 100 cases of breast carcinomas and blood samples from the same patients; they were able to amplify the viral DNA in the 21% of the breast carcinomas but not in benign breast tumors or normal breast tissues (Labracque LG, et al, 1995). After the publication of these data, many

researchers focused on the possible correlation between the presence of the EBV in breast cancer and its malignancy. A meta-analysis conducted in 2012 showed that 29.32% of the patients with breast carcinoma were positive for EBV with the highest prevalence in Asia (35.25%) and the lowest in the USA (18.27%) (Huo Q, et al., 2012). Interestingly, the analysis showed a significant increase in breast malignancy risk in patients testing positive for the EBV, suggesting that its infection is associated with increased breast carcinoma risk (Huo Q, et al., 2012).

In 2011 Mazouni found EBV DNA sequences in the 33.2% of breast cancer tissues (Mazouni C, et al., 2011). Furthermore, EBV positive tumors tended to show a more aggressive phenotype, more frequently ER negative, and with a high histological grade.

Premise and purpose of the work

Background

Microvesicles (MVs) are small extracellular vesicles physiologically secreted by different types of cells (epithelial cells, fibroblasts, hematopoietic cells, dendritic cells, T and B lymphocytes, macrophages, and others) in order to guarantee cell-to-cell communication. MVs were widely detected in various biological fluids including peripheral blood, urine and ascitic fluid; their function and composition depend on the cell from which they originate (Graves LE, et al., 2004; Piccin A, et al., 2007; Smalley DM, et al., 2008; Taylor DD, and Gercel-Taylor C, 2008). Under stress conditions like hypoxia, radiations or oxidative stress, cells tend to secrete more microvesicles and their aberrant release can arise in disease states (Ratajczak J, et al., 2006). Due to their heterogenic membrane, cargo, size, origin and function, there is not a precise categorization of the MVs thus, as of today, are divided in 3 main groups according to their size (Meckes DG, et al., 2011): 1) exosomes (40-100nm), 2) apoptotic bodies (100nm–1μm), and 3) shedding microvesicles (1–5μm). Studies over the past few years showed that MVs can contain bioactive molecules, nucleic acids and/or proteins (Cocucci E, et al., 2009) and that those packaged with miRNAs or mRNAs are mainly released from progenitors of differentiated cells and tumor cells (Ratajczak J, et al., 2006). Microvesicles shed from tumor cells facilitate transfer of soluble proteins (Iero M, et al., 2008), nucleic acids (Skog J, et al., 2008), functional trans-membrane proteins (Del Conde I, et al., 2005), chemokine receptors (Mack M. et al., 2000), tissue factors (Del Conde I, et al., 2005), and receptor tyrosine kinases (Al-Nedawi K, et al., 2008; Sanderson MP, et al., 2008). Other than *in vitro* evidence of a higher production of microvesicles by tumor cells, patients affected by cancer show a higher number of circulating MVs in the bloodstream. This can correlate with a worse prognosis of the illness (Rak J, 2010). Thus it's logical to hypothesize that there is a direct correlation between the number of invasive microvesicles, their cargo, and tumor progression.

Viral components were found in cells in which viral entry should be avoided due to the absence of specific receptors on their surface (HPV, HIV). This discovery led to hypothesize that MVs could act as mechanism of exit, transfer and entry from a permissive host cell to another.

The viral contents of microvesicles, until now, started to be investigated for HIV, hepatitis C virus (HCV), HBV, human T-lymphotropic virus (HTLV), Human Papillomavirus (HPV) and Epstein Bar Virus (EBV). In 2010 the secretion of exosomes containing functional viral miRNAs by lymphocytes B infected by EBV was demonstrated (Pegtel DM, et al., 2010). A part from another study which characterized the presence of viral DNA in apoptotic bodies coming from HPV positive cells and its transfer to primary fibroblasts (Gaiffe E, et al., 2012), little is known about the viral nucleic acids content in the microvesicles.

Oncogenic viruses are able to induce tumor formation in their natural host or in animal models. Human papillomaviruses are small epitheliotropic oncoviruses with a dsDNA of about 8 Kbps. There are 120 different HPV genotypes; between them, HPV16 and HPV18 were considered the most oncogenic ones by the International Agency for Research on Cancer (IARC). In particular, HPV16 was identified in the 60% of the high grade intraepithelial cervical dysplasia, in the 50% of the anogenital cancers and somehow in the oral, pharyngeal and lung cancers; HPV18, otherwise, is mostly associated to adenocarcinomas. Since the presence of episomal HPV DNA was only found in benign lesions, while integrated sequences of viral DNA were found in tumor tissues, this integration step has been considered fundamental for the host cell transformation process (Schneider-Maunoury S, et al., 1987). EBV is an oncovirus characterized by a linear dsDNA of approximately 172 Kbps with different internal repeat sequences (IRs) and terminal direct repeats (TRs), responsible for the circularization of the viral DNA after infection of the host. EBV is associated with the development of both lymphoid and epithelial tumors. Its role in oncogenesis was confirmed by its frequent detection in certain tumors like the Burkitt's lymphoma (BL), the post-transplant B cell lymphomas, the Hodgkin's disease (HD), the nasopharyngeal carcinoma (NPC) and the gastric cancer.

Although viral DNAs, miRNAs and proteins have been found in different types of microvesicles, the presence of viral R-loops structures in the MVs had yet to be demonstrated.

R-loops are nucleic acids structures in which a RNA strand is base paired to the template DNA strand and the non-template DNA strand remains single stranded. R-loops are necessary during the human mitochondrial DNA replication (Xu B, and Clayton DA, 1996), immunoglobulin class switch recombination (Yu K, et al., 2003), DNA methylation and post-translational histone modification (Ginno PA, et al, 2012; Nakama M, et al., 2012; Castellano-Pozo M, et al. 2013; Yang Y, et al. 2014). On the other hand, R loops can also be dangerous sources of DNA damage (Santos-Pereira JM, et al. 2013), inducing transcription's associated recombination (Huertas P, Aguilera A, 2003), or double-strand breaks (Sordet O, et al. 2009).

Other than viral nucleic acids, exosomes were shown to transfer mitochondrial DNA (Guescini M, et al., 2010), leading to the hypothesis that the nucleic acid material transferred through MVs to the recipient cells, could be imported into mitochondria.

The mitochondrial genome (mtDNA) is a closed dsDNA molecule of about 16.6 Kbs that encodes for the constituents of the enzyme complex of the oxidative phosphorylation system (Anderson S, et al., 1981; Macreadie IG, et al., 1983; Chomyn A, et al., 1985). Like genomic DNA, mtDNA can sustain mutations. Other than changes in the mtDNA, variations in its molecule number can occur; this phenomenon is linked to certain pathologic conditions and cancers: it's been demonstrated to modulate cancer initiation, cause nuclear genome instability and affect therapy response, even in breast cancer.

Breast cancer (BC) is the most common cancer in women worldwide, with nearly 1.7 million new cases diagnosed in 2012. It's been demonstrated that a third of breast cancers is related and supported by estrogens (Bajetta E, et al., 2000). Mammary cells have specific hormone receptors, particularly for progesterone and estrogen, and looks like estrogens are responsible for the induction of cells proliferation (Rana A, et al., 2010). There are many different types of BCs; the main difference between each type is the expression of estrogen receptors (ER) and progesterone receptors (PR).

Even if the mammary tissues are not primary sites of HPV infection and even if this virus is not able to induce viremia in the host, Di Leonardo discovered HPV16 DNA sequences in the 29.4% of breast tumors and some metastatic lymph nodes (Di Leonardo A, et al., 1992). A meta-analysis study conducted 20 years later (Simões PW, et al., 2012) estimated a global prevalence of HPVs in breast cancers of about the 23%. In 2004 the presence of HPV DNA sequences in breast cancer patients with a cervical pathology was discovered (Widschwendter A, et al., 2004), opening the possibility that the HPV viral nucleic acids could be transported in some way from a primary site of infection to a secondary, not permissive, tissue. The first evidence of the presence of EBV DNA in breast cancer, instead, dates back to 1995, when Labracque et al., were able to identify EBV DNA in a 21% of the samples against a 0% in benign breast tumors or normal breast tissues by PCR assay (Labracque LG, et al, 1995). A meta-analysis study conducted in 2012 (Huo Q, et al., 2012), showed that 29.32% of the patients with breast carcinoma were positive to the EBV in the tumor tissues. Interestingly, the analysis showed a significant increase in breast malignancy risk in patients testing positive for the EBV, suggesting that the viral infection was statistically associated with an increased risk of breast carcinoma (Huo Q, et al., 2012). A study conducted by Mazouni in 2011 (Mazouni C, et al., 2011) found EBV DNA in the 33.2% of the breast cancer tissues analyzed. Again, EBV positive tumors tended to show a more aggressive phenotype, more frequently ER negative and with high histological grade.

Aim of the study

Since MVs content can be transferred to recipient cells and change their phenotype, the purpose of this study was to verify if MVs could have a role in breast cancer heterogeneity and progression by the transfer of viral and mitochondrial DNA from donor to recipient cells. In fact, many studies described the presence of foreign material (viral nucleic acids or mutated mitochondrial DNA) in cancer tissues compared to normal tissues. We therefore decided to analyze the presence of viral and mitochondrial nucleic acids in MVs *in vitro* and *ex vivo*. By using cell lines positive for HPV18/16 (Hela and Caski) and EBV (Namalwa) nucleic acids, we will isolate MVs positive for viral DNAs. The quality of the microvesicles will be tested by electron microscopy and NanoSight analysis. These MVs will be used for *in vitro* and *in vivo* experiments since they will be either exposed on recipient viral-nucleic acids-negative cells or injected in breast cancer xenografts. Murine cancer associated fibroblasts (mCAFs) will be used for mtDNA transfer analysis: MVs isolated from mCAFs will be exposed on human cell lines *in vitro* in order to evaluate the transfer of the mitochondrial DNA from one cell to another. After the exposure of the recipient cells to the MVs, we will analyze the presence of viral and mitochondrial DNA by PCR and qPCR in the recipient cells in order to identify the transfer of the nucleic acids in more than one cell line model. *In vivo* experiments will be conducted in order to identify the viral DNA in the epithelial neoplastic cells and the surrounding cells, by intravenously injecting viral positive microvesides in xenografts.

We will also evaluate the presence of both viral and mitochondrial DNA in microvesicles coming from serum of patients affected by breast cancer. The specimens collected by two different hospitals, the Sant'Orsola-Malpighi Hospital, located in Bologna, Italy, which will supply specimens from newly diagnosed breast cancer patients, and the Memorial Sloan Kettering Cancer Center (MSKCC), located in New York, USA, which will give us specimens from patients affected by hormonal therapy resistant breast cancer.

The analysis on the viral DNA and RNA will be conducted for HPV16, HPV18 and EBV, since they're the most frequent viruses found in BCs. The analyses will be conducted by qPCR, PCR and colorimetric in situ hybridization (CISH). The chemical and physical structure of the viral nucleic acids in the microvesides will be investigated by nucleases treatments, PCR and qPCR and atomic force microscopy (AFM).

Materials and Methods

Cell lines and culture conditions

MCF7, ZR75, T47D, BT474 breast cancer cells lines, Caski, HeLa and Namalwa viral DNA positive cell lines (HPV16, HPV18 and EBV), were purchased from the American Type Culture Collection (ATCC). Cells were mycoplasma free. Cells were maintained in MEM or RPMI (ATCC and Media Core) supplemented with 5% fetal bovine serum (FBS, Media Core), 2 mM glutamine, 100units ml^{-1} penicillin, and 0.1mg ml^{-1} streptomycin (Media Core). Cells used for microvesicles isolation were supplemented with 5% FBS microvesicles free.
Cells were either cultured in normoxic (20% O_2, 5% CO_2) or hypoxic (1% O_2) conditions at 37°C from 3 days to a week.

Specimens

The study population was derived from two different hospitals, the Sant'Orsola-Malpighi Hospital, located in Bologna, Italy, and the Memorial Sloan Kettering Cancer Center (MSKCC), located in New York, NY, USA. The Sant'Orsola-Malpighi Hospital supplied us with 68 blood samples from newly diagnosed breast cancer patient. All individuals from the Italian hospital provided informed consent for blood donation on the approved protocol 145/2015/U/Sper. The MSKCC, instead, gave us 65 blood samples from patients affected by hormonal therapy resistant breast cancer. All individuals provided informed consent for blood donation on the MSKCC IRB-approved protocol 12-137.

Xenografts Assays

All cancer cell lines were engineered to express a GFP positive luciferase expression vector. Prior to in vivo inoculation, cancer cells were FACS sorted (for GFP) and injected bilaterally in the mammary fat pads of 5-7 weeks old non-obese diabetic/severe combined immunodeficiency mice (NOD/SCID, obtained from NCI Frederick, MD). For each in vivo experiment, cancer cells were mixed with an equal volume of Matrigel™ (BD Biosciences) in a total volume of 50µl. Bioluminescence (BLI: Xenogen, Ivis System) was used to monitor both tumour growth (weekly) and metastatic burden (at necropsy). Luminal cancer xenografts from the co-injection of human CAFs (HTR bone metastases) and MCF7 cells were also generated to determine the effect of the stroma on the generation of de novo resistant endocrine tumors. For immunostaining assays: organs were collected and fixed overnight in 4% paraformaldehyde, washed, embedded in paraffin and sectioned (Histo-Serve Core). H&E staining was performed by standard methods. For the detection of metastases at secondary sites, we performed in vivo BLI as well as immunofluorescence/immunohistochemistry staining for GFP and ER. All the surgical procedures and animal care followed the institutional guidelines and an approved protocol from our IACUC at MSKCC.

Microvesicles isolation

Microvesicles isolation from the serum coming from patients affected by hormonal therapy resistant (HTR) luminal breast cancer and the cells conditioned media was conducted following the same protocol. Briefly, the conditioned media was collected from cells grown in 10 cm dishes and centrifuged for 20' at 3,000x*g* at 4°C, as the serum. The supernatant was then transferred in ultracentrifuge tubes (Thermo Scientific) and centrifuged for 30' at 12,500x*g* at 4°C in a SW32 Ti Swinging-Bucket Rotors (Beckman Coulter). After centrifugation, the supernatant was transferred into new ultracentrifuge tubes and centrifuged at 100.000x*g* per 1.30 h at 4°C. The supernatant was discard and the pellet was washed in 1X PBS and centrifuged at 100.000x*g* per 1.30 h at 4°C. The supernatant was discarded and the microvesicles forming the pellet were resuspended in 25 µl of 1X PBS.

The pellet coming from stromal cells was further resuspended in 25 ml of 1X PBS and loaded on a 5 mls 30% sucrose cushion (300g/L sucrose, 24 g/L Tris base, pH 7.4). Samples were centrifuged at 100.000x*g* per 1.30 h at 37°C. 3.5 mls of the cushion, containing microvesicles, were transferred to a new ultracentrifuge tube, filled with 1X PBS and centrifuged at 100.000x*g* per 1.30 h at 37°C. The supernatant was discarded and the pellet resuspended in 25 µl of 1X PBS.
The microvesicles were treated or not treated, depending on the experiment, with 1 U of Baseline-ZERO™ DNase solution (Epicentre®) for 1 hr at 37°C, inactivated by an incubation at 65°C for 10', in order to get rid of the possible DNA stuck to the MVs surface or present in solution.

NanoSight analysis

Microvesicles isolated by ultracentrifugation were analyzed by using the NS500 nanopartide characterization system (NanoSight, Malvern Instruments) in order to calculate their number/ml and mean size. Briefly, 2 µl of the microvesicles resuspended in 1X PBS were diluted 1:1000 were loaded in the instrument which, thanks to a laser, analyzes the particle size, concentration, aggregation and zeta potential. Specifically, the instrument is able to quantify particle whose dimension is comprised between 100 and 1000 nm; this is the reason why we conducted electron microscopy analyses on the microvesicles as well. Results come out as a diagram file reporting the size distribution of the microvesicles, the mean size and their number.

Electron Microscopy (EM)

Microvesicles were isolated and resuspended in 20 µl 1X PBS. Cells were washed with serum-free media or appropriate buffer. Both MVs and cells were fixed with a modified Karmovsky's fix of 2.5% glutaraldehyde, 4% parafomaldehye and 0.02% picric acid in 0.1M sodium caocdylate buffer at pH 7.2 (Ito,S 1968). Following a secondary fixation in 1% osmium tetroxide, 1.5% potassium ferricyanide (De Bruijn, WC, 1973), samples were dehydrated through a graded ethanol series and embedded in an epon analog resin.
Ultrathin sections were cut using a Fiatome diamond knife (Diatome, USA, Hatfield, PA) on a Leica Ultractu S ultramicrotome (Leica, Vienna, Austria). Sections were collected on copper grids and further contrastated with lead citrate (Venable JH, and Coggeshall R, 1965.) and viewed on a JEM 1400 electron microscope (JEOL, USA, Inc., Peabody, MA) operated at 120 kV. Images were recorded with a Veleta 2K x2K digital camera (Olympus-SIS, Germany).

DNA Extraction with phenol/chloroform from cells

Cells were scraped off the plate with 2 mls of PBS and centrifuged for 5' at 1500 rpm. Supernatant was discarded and the pellet resuspended in 450 µl of tail buffer (SDS 0.5-1%, Tris-HCl 50 mM pH 8.0, EDTA 0.1 M) and 0,1 mg/ml proteinase K 20 mg/ml (ThermoFisher Scientific) and incubated O/N at 56°C. After shaking the tubes vigorously, 500 µl of phenol/chloroform (ThermoFisher Scientific) were added to each sample and centrifuged at 13,000 rpm for 5' at room temperature. The upper phase, containing the DNA was transferred to a new tube where 500 µl of chloroform were added. Samples were centrifuged at 13,000 rpm for 5' at room temperature; the DNA was washed a second time by repeating this step. The upper phase was transferred to a new tube with 450 µl of isopropanol and 50 µl of NaAc 3M. The samples were centrifuged at 13,000 rpm for 10' at 4°C. The supernatant was discarded and the pellet washed with 750 µl 70% EtOH and centrifuged at 13,000 rpm for 5' at 4°C. The DNA pellet was air dried, resuspended in 20 µl of DEPC H_2O and incubated at 37°C for 30' to allow DNA resuspension. DNA concentration was measured by loading 1 µl of DNA on a Thermo Scientific NanoDrop™ 1000 Spectrophotometer and stored at -20°C until use.

DNA extraction from microvesicles with phenol/chloroform

Microvesicles coming from ultracentrifugation were resuspended in 25 µl of 1X PBS; 500 µl of tail buffer (SDS 0.5-1%, Tris-HCl 50 mM pH 8.0, EDTA 0.1 M) and 2.5 µl proteinase K 20 mg/ml were added.
After an O/N incubation at 56°C, 500 µl of phenol/chloroform (ThermoFisher Scientific) were added to each sample. Samples were centrifuged at 13,000 rpm for 5' at room temperature. The upper phase, containing the DNA was transferred to a new tube where 500 µl of chloroform were added. Tubes were centrifuged at highest speed for 5' at room temperature. The DNA was washed a second time by repeating this step. The upper phase was then transferred to a new tube with 450 µl of isopropanol and 50 µl of NaAc 3M. The samples were centrifuged at highest speed for 10' at 4°C. The supernatant was discarded and the pellet washed with 750 µl of 70% EtOH and centrifuged at highest speed for 15' at 4°C. The DNA pellet was dried at room temperature and resuspended in 20 µl of DEPC H_2O. The DNA was incubated at 37°C for 30' to allow DNA resuspension. DNA concentration was measured by loading 1 µl of DNA on a Thermo Scientific NanoDrop™ 1000 Spectrophotometer and stored at -20°C until use.

RNA extraction from cells and microvesicles with Trizol

Cells were scraped off the plate with 2 mls of PBS and centrifuged for 5' at 1500 rpm. The supernatant was discarded and the pellet resuspended in 500 µl of Trizol (Invitrogen). Microvesicles were added with 500 µl of Trizol and mixed. The samples were centrifuged at 12,000x*g* for 30 seconds. 200 µl of chloroform were added, mixed by inversion and incubated for 2-3' at RT. After a centrifugation at 12,000xg for 15' at 4°C, the upper phase was transferred to a new tube. 400 µl of isopropanol and 3 µl of glycogen were added to the sample and incubated O/N at -20°C; the samples were then centrifuged at 12,000xg for 10' at 4°C. The supernatant was discarded and the pellet washed in 750 µl of cold 75% EtOH. The RNA was pelleted with a centrifugation at 8,000xg for 20' at 4°C, air dried and resuspended in 10 µl of DEPC H_2O. The RNA concentration was measured with a Thermo Scientific NanoDrop™ 1000 Spectrophotometer and treated for 1 hour at 37°C with 1 U (microvesicles) or 2 U (cells) of Baseline-ZERO™ DNase I (Epicentre®). RNA was stored at -80°C.

DNA extraction from cells and microvesicles by Trizol

Whenever the samples had to be analyzed by both the DNA and RNA components, DNA extraction by Trizol was performed. Cells were scraped off the plate with 2 mls of PBS and centrifuged for 5' at 1500 rpm. The supernatant was discarded and the pellet resuspended in 500 µl of Trizol (Invitrogen). Microvesicles were added with 500 µl of Trizol and mixed by pipetting up and down several times.
The samples were centrifuged at 12,000x*g* for 30 seconds. 200 µl of chloroform were added to the sample, mixed by inversion and incubated for 2-3' at room temperature. After a centrifugation at 12,000xg for 15 minutes at 4°C, the upper phase containing the RNA was transferred to a new tube and processed as described before. The remaining phases were added with 300 µl of 100 EtOH. The samples were mixed by inversion and centrifuged at 2,000xg for 5' at 4°C. The supernatant was discarded and the pellet washed in 1ml of sodium citrate/ethanol solution (0.1M sodium citrate in 10% ethanol, pH 8.5). After 30' of incubation at room temperature, samples were centrifuged at 2,000xg for 5' at 4°C. This step was repeated twice. The supernatant was discarded and 1.5 ml of 75% EtOH were added. After an incubation of 15 minutes at room temperature, samples were centrifuged at 2,000xg for 5' at 4°C. The supernatant was removed and discarded. The pellet was air dried for 5-10' at room temperature and resuspended in 20µl of 8mM NaOH. DNA concentration was measured by loading 1 µl of DNA on a Thermo Scientific NanoDrop™ 1000 Spectrophotometer and stored at -20°C until use.

Reverse Transcription PCR (RT-PCR)

Reverse transcription PCR was performed on 1 µg of RNA, previously treated with 1 U (microvesicles) or 2 U (cells) of Baseline-ZERO™ DNaseI (Epicentre®), by using with the iScript™Select cDNA synthesis Kit (Bio-Rad).
The reaction mix was prepared as following:

Reagent	**Volume (µl)**
iScript select reaction mix (5X)	2
Random primers	1
iScript reverse transcriptase	0.5
H_2O	Variable
Sample	Variable
Final Volume = 10 µl	

The reverse transcription program was the following:

Step	Temperature (°C)	Time (mins)
Hexamer Incubation	25	5
Reverse Transcription	42	60
RT Inactivation	85	5
	4	Forever

The cDNA was kept at -80°C for further analysis.

Real time PCR on DNA and cDNA

DNA and cDNA were amplified by quantitative PCR (qPCR) using the Applied Biosystem Viia™ 7 Real-Time PCR System in the Power SYBR® Green PCR Master Mix Buffer. Each sample was run in triplicate. DNA amplification was performed on 2 ng DNA/reaction; cDNA amplification was performed on 1 microliter of the cDNA/triplicate. The mix of amplification was composed as following:

Reagent	**Volume (µl)**
Power SYBR® Green PCR Master Mix 2X	5
10 µM primers mix	0.5
H_2O	3.5
Sample	1
Final Volume = 10 µl	

The amplification program was the following:

Step	Temperature (°C)	Time (secs)	Cycles
UDG Activation	50	120	1
AmpliTaq®DNA Polymerase Activation	95	120	40
Denature	95	15	
Annealing	55-60	15	
Melting	60	60	

All primers used in the Real Time assay are listed in table 1 reported in the last section of material and methods.
For analysis, ΔC_t method was applied and fold change was calculated ($2^{-\Delta\Delta Ct}$).
In order to verify the specificity of the amplicons, other than the analysis of the Melting Temperature, amplicons were visualized on a 2% agarose gel using the ChemiDoc™ XRS+ System (Bio-Rad).

Standard PCR on DNA and cDNA

The DNA and the RNA were isolated using phenol/chloroform (ThermoFisher Scientific) and Trizol (Invitrogen) respectively. Each amplification reaction was performed on a total of 20 ng of DNA or 1 µl of cDNA in a GeneAmp® PCR System 9700, version 2.5, machine. The kit used for the assay is the GoTaq®Flexi DNA Polymerase (Promega).

The amplification mix was the following:

Reagent	**Volume (µl)**
5X Colorless GoTaq® master mix	5
25 mM $MgCl_2$	2
10 µM dNTPs mix	0.5
10 µM Primers mix	0.5
5 U/µl GoTaq®Hot Start Polymerase	0.125
H_2O	15.875
Sample	1
Final Volume = 25 µl	

The amplification program performed for this assay was the following:

Step	Temperature (°C)	Time (minutes)	Cycles
GoTaq®Hot Start Polymerase Activation	95	2	1
Denaturation	95	2	40
Annealing	60	0.5	
Extension	72	1	
Final Extension	72	5	
	4	Forever	

All primers used in this assay are listed in table 1 reported in the last section of material and methods.
Thanks to special sets of primers specific for the viral sequences, we were able to discriminate between the DNA and the cDNA in one reaction; the primers used for this purpose are designed to span the intron between two exons so that the length of the DNA and cDNA amplicons are different and distinguishable when present in the same sample.
Amplicons were visualized on a 2% agarose gel using the ChemiDoc™ XRS+ System (Bio-Rad).

Long PCR

The long PCR was used in order to amplify the whole murine mitochondrial DNA using 3 pairs of overlapping primers. All primers used in this assay are listed in table 1 reported in the last section of material and methods. The 5' extremity of the primers was modified with an aminoC6 sequence so that the annealing temperature can reach 68°C and lead to a more specific amplification. Each amplification reaction was performed on a total of 20 ng of DNA with a GeneAmp®PCR System 9700, version 2.5, machine. The PCR was performed using GoTaq®Flexi DNA Polymerase (Promega) kit. The PCR master mix was composed as following:

Reagent	**Volume (µl)**
5X Colorless GoTaq® Master Mix	5
25mM $MgCl_2$	3
10 µM dNTPs mix	1.25
10 µM Forward Primer	1.25
10 µM Reverse Primer	1.25
5 U/µl GoTaq®Hot Start Polymerase	0.2
H_2O	12.05
Sample	1
Final Volume = 25 µl	

Samples were amplified using the following program:

Step	Temperature (°C)	Time (mins)	Cycles
Activation	95	2	1
Denaturation	95	3	35
Annealing	68	20	
Extension	68	10	1

Amplicons were visualized on a 0.8% agarose gel using the ChemiDoc™ XRS+ System (Bio-Rad).

DNA extraction and purification from gel

DNA amplicons resulting from PCR assays were run on gels and the bands of interest extracted using the Nucleospin®Gel and PCR clean-up (Macherey-Nagel) following manual's instruction. Amplicons were eluted in 15 µl of DEPC water and quantified at the Bioanalyzer DNA chip using the Agilent 2100 Bioanalyzer Instrument.
Samples were kept at -20°C and used for Sanger sequencing analysis of standard curve creation for copy number calculation.

Copy number quantification

Amplicons extracted by gel were quantified by QC Bioanalyzer DNA chip. The copy number of each amplicon in the eluted sample was calculated using the following formula:
Copy number = $(Ng * 6.022x10^{23}) / (Length * 1x10^{9} * 650)$
Where:
Ng = concentration of the eluted sample,
$6.022X10^{23}$ = Avogadro's number,
Length = length of amplicon in bps,
$1x10^{9} * 650$ = average weight of a base pair in ng.

After copy number quantification, we performed standard curves with serial dilutions of the amplicons of interest by qPCR assay in order to verify the quality of the amplification by CTs analysis. Data coming from qPCR assay were interpolated in the standard curve.

Microvesicles labeling and transfer to recipient cells

Microvesicles coming from murine and viral positive cells, isolated by ultracentrifugation, were labeled using the PKH67 Green Fluorescent Cell Linker Kit for General Cell Membrane Labeling (Sigma-Aldrich®). The microvesicles coming from the 1X PBS washing step were firstly resuspended in 500 µl of Diluent C and, subsequently added to a solution containing 2 µl of PKH67 and 500 µl of Diluent C. The MVs were incubated in the dark for 2-5 minutes at room temperature. The reaction was stopped by the addition of a 10% BSA solution. The unbound dye was washed by an ultracentrifugation step of 90' at 100,000x*g* at 4°C. Microvesicles were resuspended in sterile 1X PBS and exposed on cells or intravenously injected.

Before being injected in mice, microvesicles were analyzed with Nanosight and a volume containing 10^8 microvesicles was calculated in order to inject the same number of MVs in each mouse, once a week.
10^8 microvesicles were also exposed on 10^5 recipient cells grown in 8 wells cover glass Nunc®Lab-Tek®Chamber Slide (Sigma-Aldrich) in 20% O_2 and 5% CO_2. The chamber slides were incubated under an UV light for 10 minutes. 100 µl of fibronectin from bovine plasma (Sigma-Aldrich) were diluted 1:20 in PBS and incubated in the chamber slide for one hour and then removed. Cells were plated in the wells with 500 µl of growth medium.
The cells in the wells were stained with the MitoTracker® (ThermoFisher Scientific) in order to visualize the localization of the MVs in the recipient cells. Briefly, MitoTracker® was diluted 25nM in growth media and added to the cells for 30 minutes at 37°C. The solution was removed and replaced by fresh growth media added with 4% formaldehyde for 15 minutes. After fixation, cells were washed several times and analyzed.

Cryosectioning Tissues

The tumors collected from the mice were removed and cryosected. After surgery, the tumor was kept in a 4% PFA solution O/N at 4°C and then transferred to a 30% sucrose solution until the tissues sinks to the bottom. Tumor was then incubated for 1-2 hours in a 1:1 30% sucrose:OCT solution at 4°C and, to a 100% OCT solution for 1 hour, always at 4°C. Tissue was finally transferred with the 100% OCT into a mould and put on dry ice for 5 minutes avoiding the formation of bubbles.

Chromogenic In Situ hybridization (CISH)

Chromogenic *in Situ* Hybridization for HPV and EBV was performed by using the kit ZytoFast®Plus CISH Implementation Kit HRP-AEC (ZytoVision) using digoxigenin-labeled probes. Specifically, for the presence of HPV sequences in tissues was analyzed by using a probe able to recognize both the HPV16/18 DNA (ZytoFast®HPV type 16/18 Probe Digoxigenin-labeled) while the EBV was screened by using a probe directed against the EBV EBER-1 and EBER-2 RNAs (ZytoFast® EBV-CISH System). As a positive control a probe specific for the ALU sequences (ZytoFast®DNA (+) Control Probe) provided by the kit we used. All CISH analyses were performed by following the kit instructions with the only exception that the probes were incubated O/N at 37°C. Sections were visualized under a Nikon Eclipse TE300 microscope (Nikon).

Nucleases treatment of DNA from microvesicles

The DNA coming from the microvesicles isolated from cells grown both in hypoxia and normoxia was extracted and processed with different nucleases in order to analyze its chemical and physical status. After Nanodrop quantification, the samples were divided in 4 aliquots of 200 ng each, which were: 1) not treated, 2) treated with 1 U of Double-strand specific DNase (ArcticZymes®), 3) treated with 1 U of ExonucleaseS1 (New England BioLabs®), 4) treated with a combination of the two enzymes. After treatment the samples were loaded on a 1% agarose gel and visualized using a ChemiDoc™ XRS+ System (Bio-Rad).

Nucleases treatment of cellular and microvesicles RNA

The RNA coming from the cells grown in hypoxia or normoxia and from their respective microvesicles was extracted, treated with 1 U of Baseline-ZERO™ DNase (Epicentre), in order to get rid of contaminating ss- and ds-DNA, and processed with different nucleases to analyze its chemical and physical status. After Nanodrop quantification, the samples were divided in 5 aliquots of 200 ng of RNA each, which were: 1) not treated, 2) treated with 0.1mg/ml of RNase A (Thermo Scientific), 3) treated with 1 µg of ShortCut®RNase III and 1 U of RNaseH (Thermo Scientific), 4) treated with a

combination of the two enzymes and 1 U of ExonucleaseS1 (New England BioLabs®). The enzymes were inactivated by heating the samples at 65°C for 10 minutes. Specifically, these RNases digest different types of RNAs like ss- and ds-RNA (RNaseA) and RNAs present in DNA:RNA hybrid structures (RNaseH) after an incubation of 1 hour at 37°C. Enzymes were heat inactivated with an incubation of 10 minutes at 70°C.
The combination of the two enzymes would free the DNA in the DNA:RNA hybrid structures, which can be further digested by the Exonuclease S1. The DNA and the RNA present in the different RNA fractions were used for qPCR analyses in order to study the distribution of the housekeeping, mitochondrial and viral genes in the nucleic acids.
Atomic Force microscopy

The samples treated with different nucleases were analyzed by Atomic Force Microscopy, a technique that allows checking the physical status of the DNA based on the brightness and thickness of the nucleic acids. An Asylum Research MFP-3D-BIO (Oxford Instruments, Goleta CA) was used to image in tapping mode. An Olympus AC240 (Asylum Research, Goleta CA) was used for imaging. The samples were diluted to a suitable concentration in 5 mM $MgCl_2$, 25 mM HEPES pH 6.7, plated for 1-10 minutes, and washed with H_2O before being dried with N_2 gas.

DNA:RNA hybrid Immunoprecipitation (DRIP)

A concentration of 5 µg of RNA from cells was incubated overnight with 2 µg of Anti-DNA-RNA Hybrid [S9.6] Antibody (KeraFast) under rotation at 4°C in 500 µl of binding buffer (10mM $NaPO_4$ pH 7.0, 140 mM NaCl, 0.05% Triton X-100). The following day 25 µl of protein A/G magnetic beads (Pierce™) were washed twice in 500 µl of binding buffer (for 30' each wash. The RNA combined with the antibody was added to the beads and incubated for 2 hours at room temperature under rotation. 500 µl of the unbound fraction were transferred into a new 1.5 ml tube and collected for further analysis. The beads were washed twice in binding buffer for 15' at room temperature under rotation. The DNA/RNA hybrids were eluted with 250 µl of elution buffer (50 mM TRIS pH 8.0, 10 mM EDTA, 0.5% SDS) for 15' at room temperature under rotation. The elution step was repeated twice. 500 µl of phenol/chloroform (ThermoFisher Scientific) were added to both to the unbound and the bound solution and mixed by inverting the tubes. Samples were centrifuged at 13,000 rpm for 5' at room temperature and the upper phase collected. 400 µl of isopropanol and 3 µl of glycogen were added and mixed by inverting the tubes. Samples were incubate overnight at -20°C. The tubes were incubated for 10 minutes at room temperature and centrifuged at 12,000x*g* for 10' at 4°C. The supernatant was discarded and the pellet was washed in 750 µl of 75% EtOH. RNA was precipitated by centrifugation at 8,000xg for 10' at 4°C. Supernatant was removed, pellet was resuspended in 8 µl of DEPC H_2O and incubated for 5' at 65°C. RNA concentration was measured by loading 1 µl of DNA on a Nanodrop;1000 Spectrophotometer. Samples were stored at -80°C.

Statistical analysis

Statistical analysis was performed by SPSS (SPSS Incorporation). Continuous variables were analyzed by unequal variance t-test, paired t-test (samples, n=2), general linear model (GLM) Anova or GLM for repeated measures (samples, n>2). Mann-Whitney, Wilcoxon and Friedman tests were used to analyze ordinal variables. P values were adjusted for multiple comparisons according to Bonferroni correction. Association among quantitative variables was quantified by Pearson correlation coefficient. Categorical variables were analyzed by Fisher exact test or Monte Carlo $\chi 2$ test. All the tests were two-sided. $P<0.05$ was considered significant. Elda software was used to measure the statistics of limiting dilution experiments.

Primer Tables

The reference sequences used for primers design are NC_010339 for the murine mitochondrial DNA, NC_012920 for the Human mitochondrial DNA, NG_007992 for the human Beta Actin, NG_007073.2 for the human GAPDH, NM_007393.5 for the murine Beta Actin, NC_001357.1 for Human Papillomavirus type 18, NC_001526 for Human Papillomavirus type 16, NC_007605 for Epstein Barr Virus.

Table1: Murine Mitochondrial Primers

Murine Mitochondrial DNA					
Gene	**Sequence 5'-3'**	**Position**	**Length (bps)**	**Assay**	**Reference**
DLoop	AGGTTTGGTCCTGGCCTTAT	72 F	149	Real Time	SnapeGene Viewer Software
	GTGGCTAGGCAAGGTGTCTT	221 R			
12S	CTAGCCACACCCCCACGGGA	214 F	114		
	CGTATGACCGCGGTGGCTGG	328 R			
16S	CGGCAAACAAGAACCCCGCC	1912 F	108		
	GTCAGGATACCGCGGCCGTT	2020 R			
ND1	CAGCCGGCCCATTCGCGTTA	3398 F	197		
	AGCGGAAGCGTGGATAGGATGC	3595 R			
ND2	TCCTCCTGGCCATCGTACTCAACT	4123 F	131		
	AGAAGTGGAATGGGGCGAGGC	4254 R			
COX1	CCAGTGCTAGCCGCAGGCAT	5927 F	127		
	TCTGGGTGCCCAAAGAATCAGAACA	6054 R			
COX2	AGTTGATAACCGAGTCGTTCTGCCA	7425 F	123		
	TCGGCCTGGGATGGCATCAGT	7548 R			
ATP6	GCTCTCACTCGCCCACTTCCTTCC	8297 F	529		
	GCCGGACTGCTAATGCCATTGGTT	8826 R			
COX3	ACCTACCAAGGCCACCACACTCC	8804 F	149		
	GCAGCCTCCTAGATCATGTGTTGGT	8953 R			
ND3	ACCCTACAAGCTCTGCACGCC	9585 F	385		
	GCTCATGGTAGTGAAGTAGAAGGGCA	9970 R			
ND4 L	TCGCTCCCACCTAATATCCACATTGC	9945 F	141		
	GCAGGCTGCGAAAACCAAGATGG	10086 R			
ND4	TCGCCTACTCCTCAGTTAGCCACA	11026 F	115		
	TGATGATGTGAGGCCATGTGCGA	11141 R			
ND5	TCGGAAGCCTCGCCCTCACA	12868 F	105		
	AGTAGGGCTCAGGCGTTGGTGT	12973 R			
ND6	AATACCCGCAAACAAAGATCACCCAG	13585 F	99		
	TGTTGGGGTTATGTTAGAGGGAGGGA	13684 R			
Cytb	ACAGCAAACGGAGCCTCAA	14394 F	134		
	TGCTGTGGCTATGACTGCGAACA	14528 R			

Table 2: Human Mitochondrial Primers

Human Mitochondrial DNA					
Gene	**Sequence 5'-3'**	**Position**	**Length (bps)**	**Assay**	**Reference**
DLoop	TGGCCACAGCACTTAAACACATCTC	321 F	175	Real Time	SnapGene Viewer Software
	GGGTTGTATTGATGAGATTAGTAGTATGGGAG	496 R			
12S	CCCGTTCCAGTGAGTTCACCC	706 F	221		
	CTATTGACTTGGGTTAATCGTGTGACC	927 R			
16S	AACTTTGCAAGGAGAGCCAAAGC	1873 F	205		
	GGGATTTAGAGGGTTCTGTGGGC	2078 R			
ND1	ACGCCATAAAACTCTTCACCAAAG	3458 F	103	Real Time/PCR	
	TAGTAGAAGAGCGATGGTGAGAGCTA	3561 R			
ND2	CTTCTGAGTCCCAGAGGTTACCCA	4805 F	182	Real Time	
	CCGTCAACTCCACCTAATTTGGTTTG	4987 R			
COX1	TGCCATAACCCAATACCAAACGC	6425 F	112		
	CTGTTAGTAGTATAGTGATGCCAGCAGCTAGG	6537 R			
COX2	CTACGGTCAATGCTCTGAAATCTGTG	8161 F	153		
	GCTAAGTTAGCTTTACAGTGGGCTCTAG	8314 R			
ATP6	GAAAATCTGTTCGCTTCATTCATTGCC	8533 F	138		
	GCTGATTAGTGGTGGGTTGTTACTG	8671 R			
COX3	CGATACGGGATAATCCTATTTATTACCTCAG	9444 F	199		
	CAGGTGATTGATACTCCTGATGCGA	9643 R			
ND3	CATTTTGACTACCACAACTCAACGGCTAC	10120 F	160		
	GGGTAAAAGGAGGGCAATTTCTAGATC	10280 R			
ND4L	GCTACTCTCATAACCCTCAACACCC	10599 F	130		
	AGGCCATATGTGTTGGAGATTGAGA	10729 R			
ND4	CCAACGCCACTTATCCAGTG	10999 F	237		
	GGGAAGGGAGCCTACTAGGGTGT	11236 R			
ND5	TTACCACCCTCGTTAACCCTAACAAA	12395 F	165	Real Time/PCR	
	TGGGTTGTTTGGGTTGTGGCT	12560 R			
ND6	ACGCCCATAATCATACAAAGCCC	14224 F	149	Real Time	
	GGATTGGTGCTGTGGGTGAAA	14373 R			
Cyt-b	CGCCTGCCTGATCCTCCAA	14860 F	191		
	AGGCCTCGCCCGATGTGTAG	15051 R			
Mito 1	[aminoC6]ACATAGCACATTACAGTCAAATCCCTTCTCGTCCCC	16331 F	3968	Long PCR	Dames S., et al., 2015
	[aminoC6]TGAGATTGTTTGGGCTACTGCTCGCAGTGC	3729 R			
Mito 2	[aminoC6]TACTCAATCCTCTGATCAGGGTGAGCATCAAACTC	3646 F	5513		
	[aminoC6]GCTTGGATTAAGGCGACAGCGATTTCTAGGATAGT	9458 R			
Mito 3	[aminoC6]TCATTTTTATTGCCACAACTAACCTCCTCGGACTC	8753 F	9289		
	[aminoC6]CGTGATGTCTTATTTAAGGGGAACGTGTGGGCTAT	16566 R			

Table 3: Housekeeping Primers

Housekeeping Genes						
Gene	**Sequence**	**Position**	**Length (bps)**	**Assay**	**Target**	**Reference**
ACTB	AGGATCTTCATGAGGTAGTCAGTCAG	1358 F	98	Real Time	DNA	Clone Manager 9 (Sci-Ed Software)
	CCACACTGTGCCCATCTACG	1456 R				
GAPDH	CTCTGCTCCTCCTGTTCGAC	5030 F	126	Real Time/PCR	DNA	SnapGene Viewer Software
	CGCCCGCGTCCGGCCTACACA	5156 R				
ACTB	ACCAACTGGGACGACATGGAG	313 F	379	Real Time/PCR	RNA	Clone Manager 9 (Sci-Ed Software)
	GTGGTGGTGAAGCTGTAGCC	692 R				

Table 4: HPV 18 Primers

Human Papillomavirus 18						
Gene	**Sequence 5'-3'**	**Position**	**Length (bps)**	**Assay**	**Target**	**Reference**
E7	GAAAGCTCAGCAGACGACCT	818 F	62	Real Time	DNA	Clone Manager 9 (Sci-Ed Software)
	CACAAAGGACAGGGTGTTCA	880 R				
E6	TGCACGGAACTGAACACTTCAC	156 F	345	PCR		
	GCCCAGCTATGTTGTGAAATCG	501 R				
	GGTGCCAGAAACCGTTGAATC	424 F	77	Real Time/Nested PCR		
	GCCCAGCTATGTTGTGAAATCG	501 R				
	ATCCAACACGGCGACCCTAC	121 F	295/112	PCR	DNA/RNA	
	ACCGCAGGCACCTCTGTAAG	233^416 R				

Table 5: HPV 16 Primers

Human Papillomavirus 16						
Gene	**Sequence 5'-3'**	**Position**	**Length (bps)**	**Assay**	**Target**	**Reference**
E7	CAACTGATCTCTACTGTTATGAGCAA	617 F	72	Real Time	DNA	Clone Manager 9
	CCAGCTGGACCATCTATTTCA	689 R				(Sci-Ed Software)
E6	CAACAGTTACTGCGACGTGAG	206 F	348	PCR		
	GCTGGGTTTCTCTACGTGTTC	554 R				
	CAACAGTTACTGCGACGTGAG	206 F	218	Nested PCR		
	AAAGCCACTGTGTCCTGAAGA	424 R				

Table 6: EBV Primers

Epstein Barr Virus						
Gene	**Sequence 5'-3'**	**Position**	**Length (bps)**	**Assay**	**Target**	**Reference**
LMP2	CTTGGAGACAGGCTTAACCAGACTCA	71232	264	Real Time	DNA	SnapGene Viewer Software
	CCATGGCTGCACCGATGAAAGTTAT	71496				
LMP1	AAGGCCAAAAGCTGCCAGATGGTGGC	168435	168/92	PCR	DNA/RNA	
	ATCTTCGGGTGCTTACTTG	168602				

Results

Microvesicles analysis

Microvesicles coming from HPV positive cancer cell lines and murine stromal cell lines undergoing up to 3 rounds of hypoxia (1% O_2, 4 days, H) and re-oxygenation (20% O_2, 3 days, R) were isolated by ultracentrifugation. Specifically, cells were firstly cultured in normoxic conditions for 3 days and then in hypoxic conditions for 4 days. These steps were repeated three times and after each cycle of HR the microvesicles were collected. A schematic representation of the HR treatments is shown in figure 1.

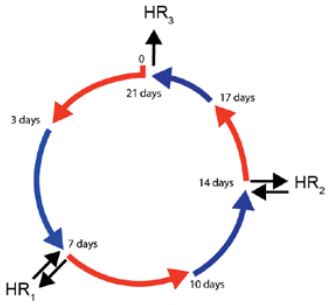

Figure 1: Schematic representation of MVs collection. Cells are grown in normoxic conditions (20%O_2) for 3 days and then transferred to hypoxic conditions (1% O_2) for 4 days. After each HR round MVs were collected by ultracentrifugation, up to 3 rounds

The number and quality of the MVs isolated in normoxic and hypoxic conditions were evaluated by NanoSight and electron microscopy. By NanoSight analysis we got information about the size and the number of microvesicles per ml. In figure 2 we report a Nanosight diagram of microvesicles coming from cells cultured in normoxic and hypoxic conditions; in hypoxia, cells released larger MVs whereas the number is almost doubled, compared to cells from normoxic culture conditions.

Normoxia:

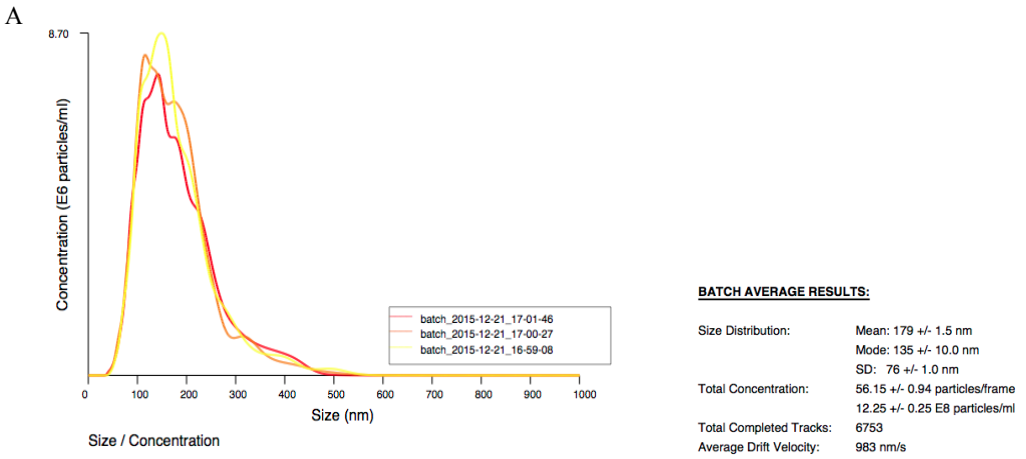

Hypoxia:

B

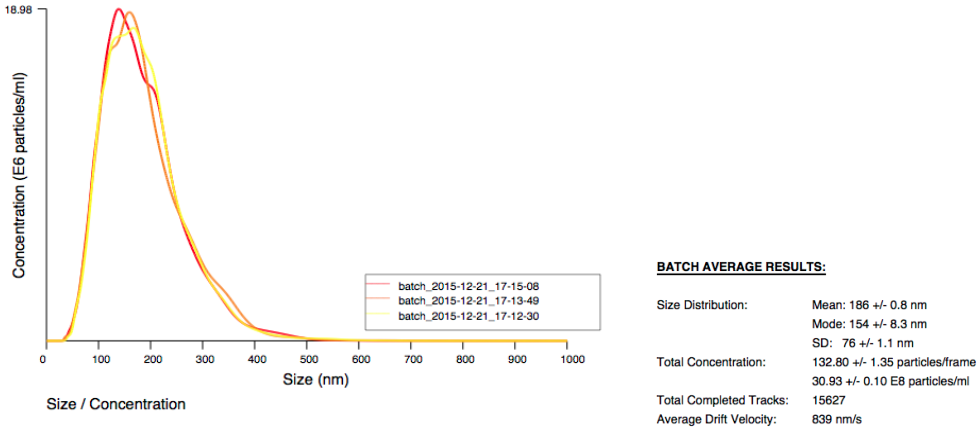

Figure 2: **Nanosight diagram of MVs collected from cells cultured in normoxic or hypoxic conditions.** (**A**) MVs coming from normoxic conditions show a lower number and a mean distribution size almost identical compared to (**B**) MVs coming from cells cultured in hypoxic conditions, in which the number is more than doubled.

We also analyzed the MVs coming from the blood of patients affected by a hormonal therapy resistant (HTR) breast cancer, by NanoSight (Figure 3). The result showed that they have a larger mean size compared to microvesicles coming from our cell lines (192 nm vs. 179-186 nm); their number is around $3x10^8$ when 5 ml of serum are centrifuged.

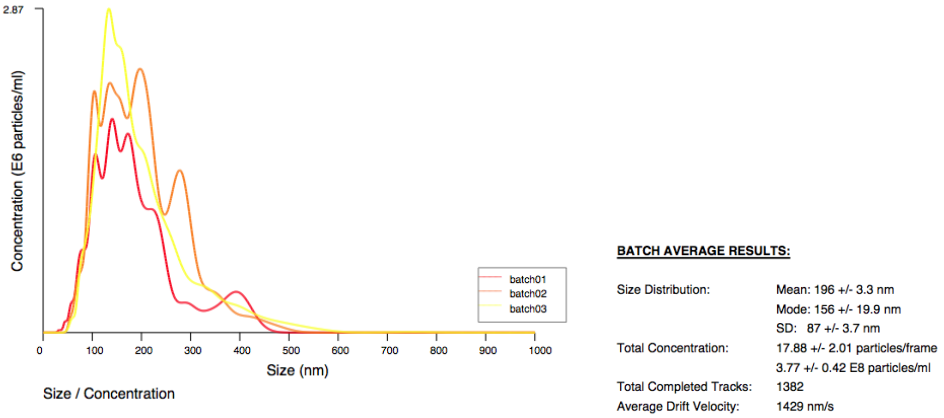

Figure 3: NanoSight diagram of microvesicles isolated from blood of a patient with hormonal therapy resistant breast cancer. Microvesicles isolated by ultracentrifugation show a larger size compared to the MVs coming from cells grown in normoxic or hypoxic conditions. Their number is almost the same when 5 mls of serum are ultracentrifuged.

By electron microscopy, we were able to determine the quality of the microvesicles isolated by ultracentrifugation (Figure 4). As by NanoSight, the presence of microvesicles isolated from 10^6 Caski cancer cells (left picture) and from the patients blood was demonstrated (right picture).

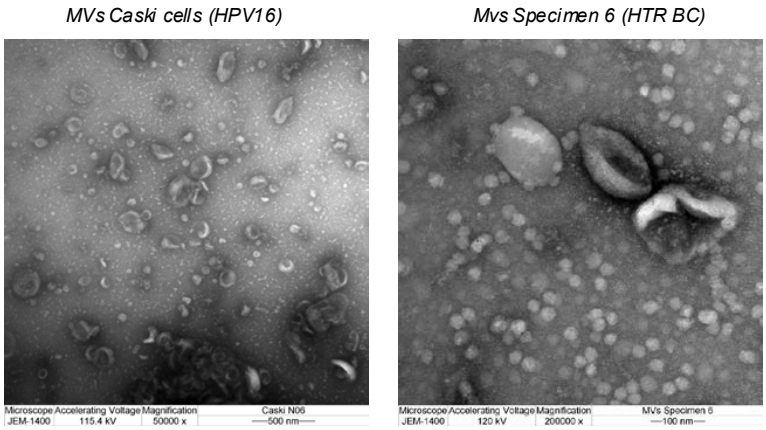

Figure 4: Electron microscopy of MVs coming from Caski cell line (HPV16 positive) and from the blood of a patient with HTR breast cancer. The presence of MVs coming from Caski cell line and from the blood of a patient affected by HTR breast cancer is checked by electron microscopy anamysis. From the pictures we could notice that MVs coming from the blood show less size variability compared to the MVs coming from the cell line.

Viral and mitochondrial DNA sequences in microvesicles

Once we analyzed the quality of our microvesicles, we proceeded with the molecular analyses. First of all we determined the DNA concentration in microvesicles treated or not treated with DNaseI, an enzyme able to digest ssDNA and dsDNA, prior DNA extraction. The results are shown in figure 5. All cell lines, even if with some differences, showed a drop in the DNA concentration after DNaseI treatment. This led to the conclusion that some free DNA can be stuck on the microvesicles membrane and not being internalized in the MVs. After this result, all experiments were conducted with MVs treated with DNaseI prior each nucleic acids extraction, injection or exposure on cells to be sure that the DNA eventually amplified or transferred, was inside the microvesicles and not outside and to devoid for DNA contamination (free DNA in the media).

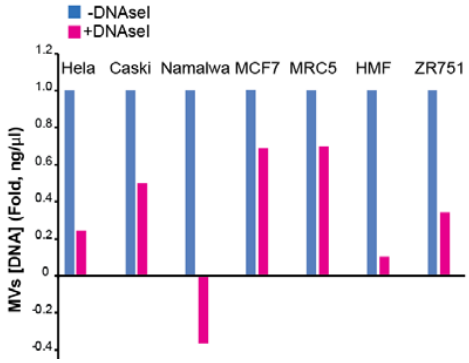

Figure 5: Presence of free DNA molecules on the MVs membrane. MVs isolated by ultracentrifugation from tumor cells (HeLa, Caski, Namalwa, MCF7, ZR751) or fibroblasts (MRC5, HMF), were treated or not treated with DNAseI before DNA extraction. The [DNA] of MVs treated with DNaseI was lower compared to MVs not treated indicating the presence of free DNA molecules on the MVs membranes.

Since many evidences either from literature or from our results, showed an increase in the MVs number when cells undergo HR treatments, we wanted to evaluate if even the DNA concentration in those microvesicles was higher. The DNA inside MVs coming from cells undergoing HR treatments was extracted and quantified by Nanodrop; as reported in figure 6, the DNA concentration/μl resulted higher in microvesicles coming from cells that underwent 3 rounds of HR treatment compared to cells cultured in normoxia or that underwent 1 or 2 rounds of HR treatments. Even if both Caski and HeLa cells are HPV positive cancer cells, there's a big difference in their MVs content; undergoing the same HR treatments, Caski cells showed a constant increment of the DNA concentration in the microvesicles, while HeLa cells show a raise in DNA concentration only after the third round of HR treatment.

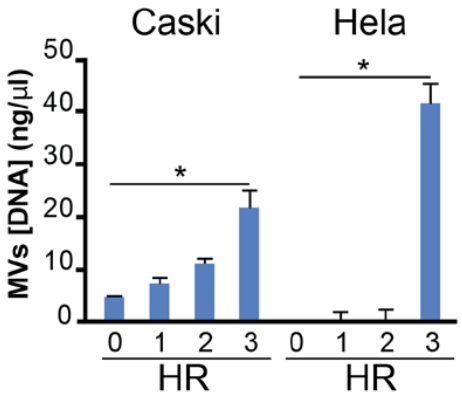

Figure 6: HR treatments increase the concentration of the DNA inside the MVs during time. The DNA concentration of microvesicles isolated from Caski and HeLa cells cultured under HR treatments during 3 weeks was evaluated. After 3 weeks of treatments the DNA concentration was constantly increased in Caski of about 5 times. In HeLa cells the DNA concentration suddenly increased of 40 times after the third round of HR treatments.

The presence of the viral and genomic DNA was demonstrated by qPCR. In figure 7 we report a bar graph indicating the copy number variation of GAPDH, Beta Actin and HPV DNA in Caski and HeLa cells cultured in normoxic conditions or after 3 rounds of HR treatments. As showed previously, the copy number increases after the HR treatments compared to the normoxic ones.

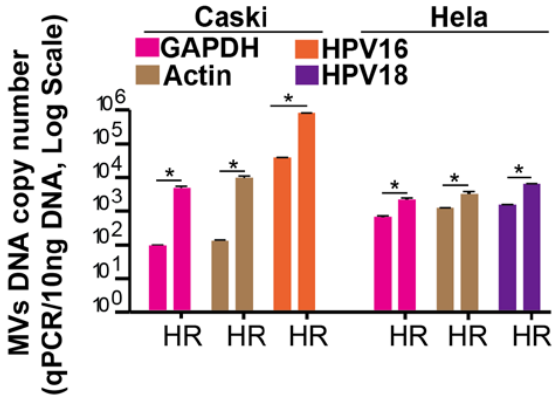

Figure 7: Presence of viral and genomic DNA in MVs coming from HPV positive cell lines. A qPCR for the human GAPDH, Beta Actin and HPV DNAs in MVs was performed in order to calculate their copies number in normoxic or HR MVs. The amount of genomic and viral DNA increases in HR MVs mostly in the Caski cells compared to the HeLa.

Once we analyzed the presence and the copy number of viral and genomic DNA in the MVs, we compared the DNA copy number in HR MVs compared to the cells from which they come from (Figure 8). While the copy number of the genomic genes in the cells and MVs was almost the same in the HPV16 positive (Caski), HPV18 positive (HeLa) and the EBV positive (Namalwa) cells, the viral copy number changed more, maybe because of the different sites of viral DNA integration in the cells.

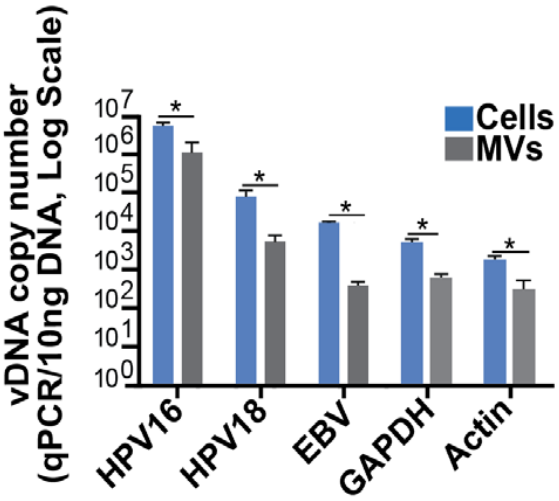

Figure 8: High variation in the viral genes copy number between cells and their MVs, compared to the genomic ones. The genomic DNA copy number calculation of viral and genomic DNA sequences in cells versus their respective microvesicles was calculated after qPCR amplification. Housekeeping's gene copy number is reported as a mean of the two cell lines

Human fibroblasts (hCAFs) and cancer cells (Caski) were tested for the presence of mitochondrial DNA (mtDNA) by qPCR in MVs treated or not treated with DNaseI prior DNA extraction. Figure 9 shows how, after DNAseI treatment, the ratio between the mtDNA and the nuclear DNA (nDNA) increases, leading to the conclusion that the mtDNA was mostly present inside the MVs.

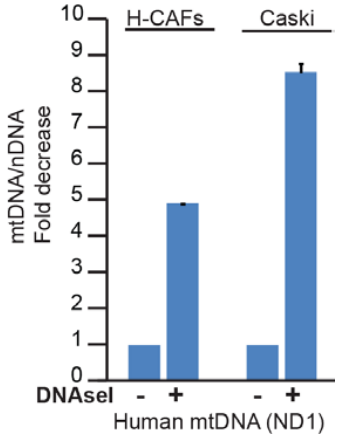

Figure 9: Presence of mitochondrial (ND1) and nuclear (GAPDH) DNA in MVs. MVs isolated from human fibroblasts and cancer cells were treated or not treated with DNaseI prior DNA extraction. After treatment, the ratio between the mtDNA and the nDNA increases mostly in the cancer cell lines meaning that, in these cells, the mtDNA is enriched in MVs coming from cancer cells compared to the nDNA.

Other than a real time assay, the presence of the mitochondrial DNA in the MVs was also evaluated by PCR. All mitochondrial genes were screened in MVs coming from HR HeLa cells. After amplification we loaded the samples on a 2% agarose gel, showed in figure 10.

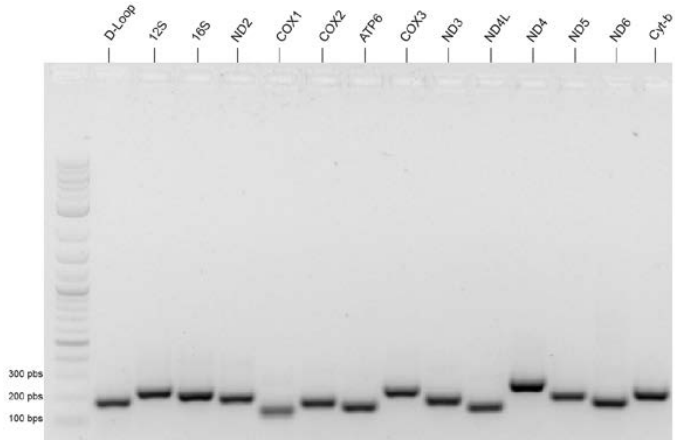

Figure 10: All mitochondrial genes are present in the HR MVs coming from HeLa cells. HR MVs coming from HeLa cells were isolated by ultracentrifugation and treated with DNaseI followed by DNA extraction. The DNA inside the MVs was amplified with 14 primer pairs, covering the complete mtDNA genome.

Given this result, we wondered if other than a fragmented DNA, a complete circular mitochondrial DNA was present in the MVs. Therefore, we amplified the DNA coming from both the cells and the resulting MVs using three overlapping primers pairs, which permitted the amplification of the entire mtDNA. The primers used in this screen gave rise to amplicons of about 4, 5 and 9 Kbs. We were able to amplify the third region with a really lower efficiency compared to the other two regions in both the cells and the MVs, probably because the excessive length of the amplicon.
In figure 11 we show an example of long PCR amplification on HeLa cells.

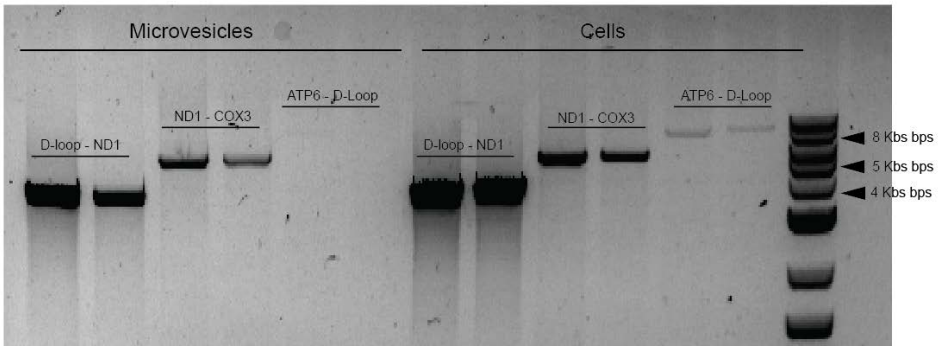

Figure 11: Presence of possibly entire, circular mtDNA molecules in the MVs. A Long PCR assay on mtDNA in microvesicles coming from HeLa HR MVs and cells was performed. The primers covered the regions comprised between the D-loop and the ND1 (3968 bps), the ND1 and the COX3 (5513 bps) and the ATP6 and the D-loop (9289 bps).

The specificity of the viral DNAs and the mtDNA in the microvesides was confirmed by sequencing. In Figure 12 we report an example of sequencing diagram of the LMP2 EBV amplicon deriving from MVs isolated from Namalwa cells.

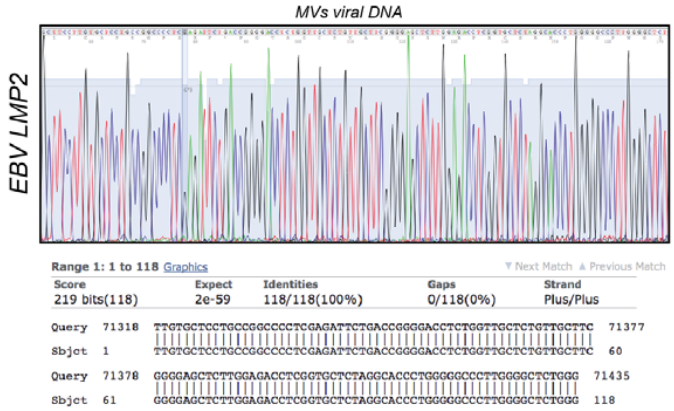

Figure 12: Sequencing of the LMP2 EBV gene. The viral and mitochondrial products of amplification were loaded on an agarose gel, extracted and sequenced. The sequenced was then blasted with the reference sequence on PubMed.

Viral and mitochondrial DNA transfer by microvesicles *in vitro*

Once we established that both the viral and the mitochondrial DNA sequences were present in the MVs, we performed in vitro experiments in order to evaluate if the DNA could be transferred to recipient cells. Viral negative recipient cells were exposed to fluorescent labeled MVs isolated from Caski, HeLa and Namalwa cells that underwent HR treatments. After 2 hours of exposure we looked at the recipient cells by confocal microscopy and saw that, while the fibroblasts were already positive for the MVs staining, cancer cells were still negative. After 12 hours also the epithelial cells became positive for the MVs staining. In figure 13 we show two pictures took by confocal microscopy of both fibroblasts and cancer cells positive to the MVs. In order to visualize the cellular compartment in which the MVs were up taken, we used MitoTracker (red) to trace the mitochondria, DAPI (blue) to visualize the nuclei and PKH67 cellular linker (green) for the MVs. In this way we were able to visualize the MVs co-localization with the mitochondrial compartment and the nucleus. By this analysis we were able to see that while the microvesicles up taken by fibroblasts were mainly localize in the mitochondrial compartment, the microvesicles in the cancer cells were localized both in the nucleus and the mitochondria.

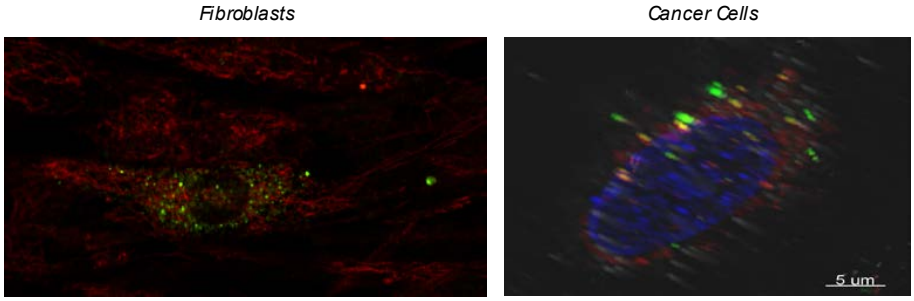

Figure 13: Transfer of HeLa HR MVs to fibroblasts and cancer cells *in vitro*. Fibroblasts and cancer cells were exposed to HR HeLa MVs. Fibroblasts exposed to MVs showed a high up take after only 2 hours while cancer cells turned positive after 12 hours. MVs are mainly present in the cytoplasm of the fibroblasts while are almost equally distributed between the cytoplasm and the nucleus in the cancer cells.

The viral and mitochondrial DNA transfer was evaluated by PCR and qPCR. In order to evaluate if there was any difference between the transfer of nucleic acids from hypoxic or normoxic MVs to recipient cells, we exposed recipient cells (10^5 cells) to MVs (10^8 particles) every 48 hours for a week. As reported in figure 14, the recipient cells exposed to MVs derived from HR cells, show a higher viral DNA copy number compared to those which received the normoxic MVs. We exposed two cancer cell lines (MCF7 and ZR751) and one human fibroblast cell line (BR11) to the MVs coming from normoxic and hypoxic Namalwa cells (EBV positive) and evaluated the viral copy number in the recipient cells after 24 hours post exposure; we saw that 1) the viral DNA copy number in the fibroblasts was higher compared to the cancer cells and 2) the viral DNA copy number in cells exposed to normoxic MVs was almost zero compared to the viral copy number in cells exposed to HR MVs.

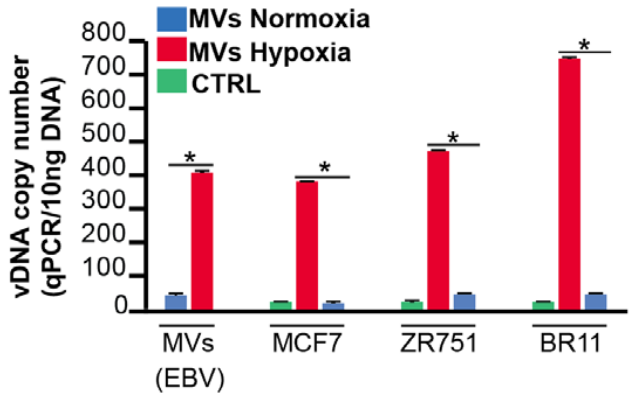

Figure 14: Viral DNA transfer to recipient cells through MVs. Normoxic and HR EBV positive microvesicles were isolated by ultracentrifugation, treated with DNaseI, and bumped on both viral negative cancer cells and fibroblasts every 48 hours for a week. After 7 days, the cells were washed in 1X PBS and the DNA was extracted. Cells exposed to HR microvesicles show a higher number of viral copy number compared to those exposed to normoxic MVs. Also, the viral copy number in fibroblasts is higher than in the cancer cells, in which is almost the same between three different cell lines.

The transfer of the mitochondrial DNA was evaluated exposing human mammary cancer cells (BT474) to MVs coming from murine cancer associated fibroblasts (mCAFs). By using primers that targeted all the mitochondrial genes, we were able to amplify the whole mitochondrial genome, meaning that the mtDNA was transferred. As reported in figure 15, we weren't able to amplify the murine genomic genes (COX4 and β2M).

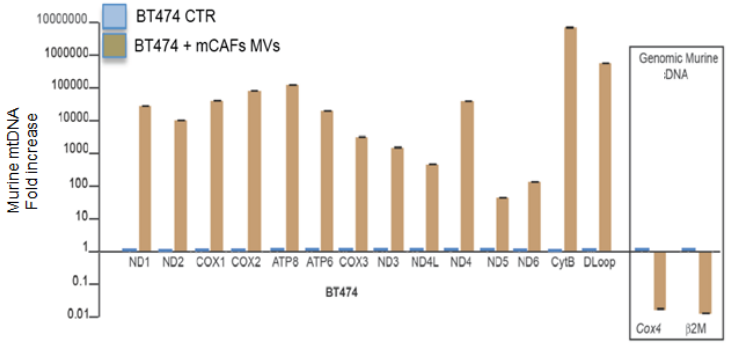

Figure 15: mtDNA transfer to recipient cells through MVs. MVs from murine CAFs were treated with DNaseI and dumped on BT474 cells. The transfer of the murine mtDNA to human recipient cells was evaluated by amplifying all the murine mitochondrial genes by qPCR.

Viral nucleic acids transfer through microvesicles *in vivo*

The positive results in vitro prompted us to analyze the transfer of viral DNA sequences in vivo. We injected 10^6 MVs from Caski, HeLa and Namalwa cells 4 times/month in the arterial circulation of mice bearing luminal breast cancer xenografts (MCF7 or ZR751 cells). Following a period of 5 months of MVs education mice were sacrificed. By colorimetric in situ hybridization (CISH) and PCR we were able to identify HPV DNA (E6 and E7) and EBV RNA (EBER1) sequences in tissues, including cancer cells and fibroblasts, both in primary tumor and in the metastatic microenvironment. In figure 16 the positivity to the HPV, EBV sequences is shown.

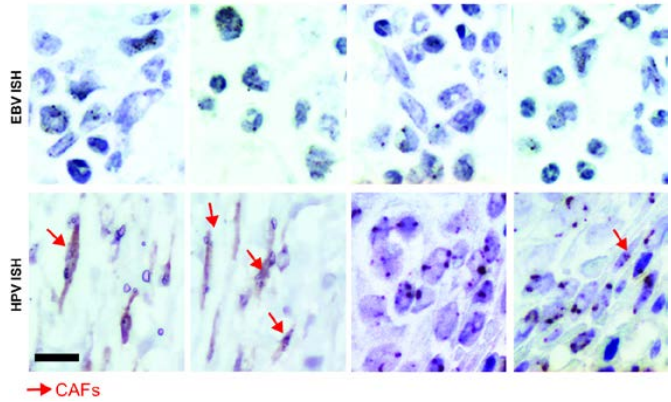

Figure 16: Transfer of viral nucleic acids through microvesicles, *in vivo*. MVs isolated from HPV and EBV positive cell lines. After NanoSight analysis, 10^6 MVs were treated with DNaseI and intravenously injected in breast cancer xenografts. The HPV DNA and the EBV RNA from viral positive MVs in xenografts was identified by CISH in the tumor and in some murine fibroblasts surrounding the tumor.

Analysis of viral and mitochondrial DNA in *ex vivo* microvesicles

To translate our discovery to patient-derived specimens, we isolated MVs from two distinct breast cancer cohorts and analyzed the presence of HPV DNA sequences by qPCR. The results on the MVs isolated by newly diagnosed breast cancer patients, showed the presence of HPV DNA in the 11% of the total MVs (8/68), with a 6% of positivity for the HPV18 (4/68), a 4% to the HPV16 (3/68) and a 1% of positivity to the HPV31 (1/68). When the analysis was conducted on MVs coming from patients affected by hormonal therapy resistant breast cancer, the results showed a total positivity of the 14% (9/65) with a 6% positive for the HPV16 (4/65), a 5% positive for the HPV18 (3/65), and a 3% of co-infection of HPV16 and HPV18 (2/65). These data are summarized in figure 17.

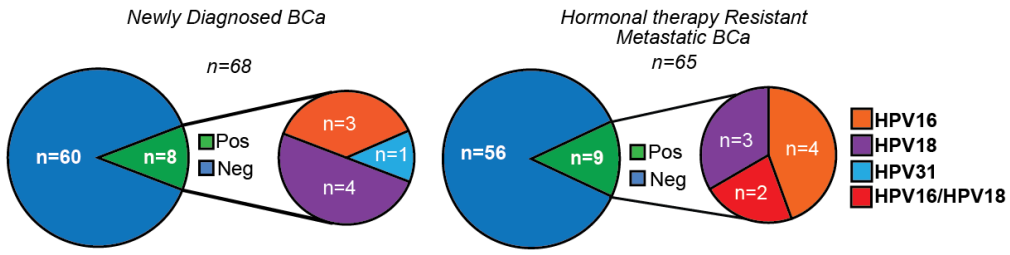

Figure 17: Presence of HPV DNA sequences in MVs coming from the blood of patients affected by breast cancer. MVs coming from the circulation of newly diagnosed breast cancer patients and affected by HTR breast cancer were treated with DNaseI. The DNA was extracted and screened for the presence of the E6 region of the HPV by PCR and qPCR.

The HPV16/18 DNA copy number was evaluated in the HTR cohort only and is shown in figure 18.

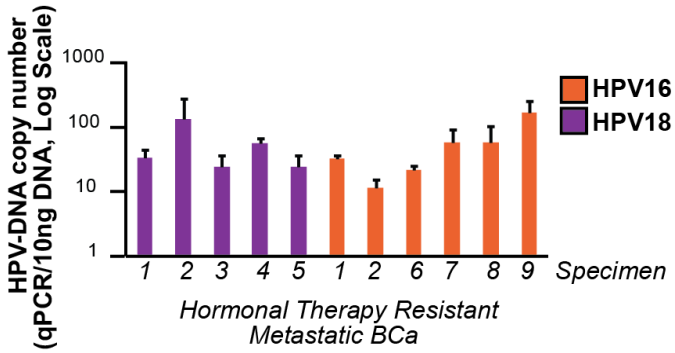

Figure 18: Copy number evaluation of the HPV18 and HPV16 DNA in the circulating MVs of patients affected by HTR breast cancer. The copy number of the viral DNA amplified in the MVs of patients affected by HTR breast cancer was evaluated after amplification by qPCR.

Other than the HPV DNA analysis, the presence of GAPDH and ND1 was evaluated by qPCR in the HTR cohort. GAPDH DNA sequences where found in the 36% of the microvesicles (26/72) while the mitochondrial ND1 gene was amplified in the 72% of the microvesicles (52/72).

Analysis of the chemical-physical status of nucleic acids in MVs

The presence of the viral RNA in MVs coming from HeLa, Caski and Namalwa cells was analyzed by PCR. To analyze the presence of the RNA, we used primers able to amplify both the DNA and the RNA at the same time since they are designed to span an intron and they give rise to amplicons of different lengths. Although we were able to identify the viral RNA in the MVs, we also noticed that, even after DNaseI treatment of the RNA prior retro-transcription, we were amplifying viral DNA. The presence of both the viral DNA and the cDNA in the MVs coming from HR HeLa but not in the cells is shown in figure 19.

Figure 19: Presence of DNaseI resistant viral DNA in the RNA fraction of HR MVs. The RNA coming from HR viral positive MVs and cells was extracted and treated with DNaseI prior retro-transcription. By using primers able to amplify both the RNA and the possible contaminating DNA we were able to identify some viral DNA resistant to the nuclease's treatment.

Since this result was mainly obtained in HR MVs than in normoxic MVs, we hypothesized that the nuclease's resistant DNA could be incorporated in a more complex structure, like an R-loop, known to be more synthesized in hypoxic conditions. Therefore, we analyzed the physical and chemical status of the DNA in the RNA fraction by using different nucleases. In figure 20 the viral DNA copy number amplified in the RNA treated with different nucleases is shown. The nDNA sequences in the RNA fraction were mostly characterized by dsDNA since after DNaseI treatment they showed a drastic drop in their copy number. At the contrary, the viral DNA sequences persisted after DNaseI treatment and were mostly eliminated after RNaseH treatment (which digests the RNA in the R-loop structure) and ExonucleaseS1 digestion (which digests the ssDNA), which supports the hypothesis that viral DNA could be protected by a more complex structure.

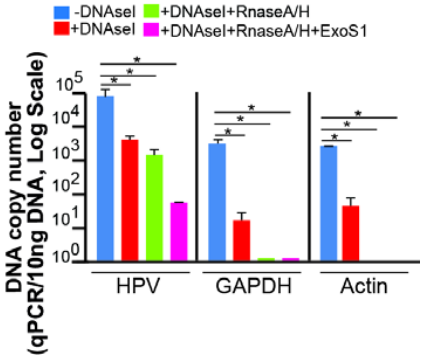

Figure 20: Presence of viral DNA complexes in R-loop structures in HR HeLa MVs. RNA was extracted from HR viral positive MVs and not treated with DNaseI (blue), treated with DNaseI (red), treated with DNaseI, RNaseA and H (green) and treated with DNaseI RNaseA and H and ExonucleaseS1 (pink). The viral DNA copy number shows a drop in after treatment with both the RNases and the Exonuclese S1. The nDNA, instead, shows a drop mainly after DNaseI treatment.

Since microvesicles coming from cells grown in normoxia or hypoxia showed different concentration of DNA (Figure 6), we wanted to evaluate if even the chemical-physical status of the DNA in the MVs was different. To do that, we performed nucleases treatments on normoxic or hypoxic HeLa MVs and did the qPCR on the viral DNA. In figure 21 the viral copy number is shown. As reported in the figure, the viral copy number in the hypoxic MVs showed a drop after treatment with RNAseA/H and Exonucleasel. In the normoxic MVs, instead, the copy number after these treatments remained almost the same. This result means that the viral DNA in the hypoxic MVs is combined with some RNAs in a more complex structure while the viral DNA in the normoxic MVs seems to be a dsDNA, since after DNaseI treatment the drop is more evident.

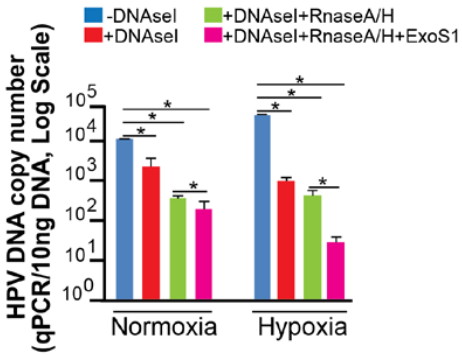

Figure 21: HR MVs have show a prevalence of viral DNA complexes in R-loops compared to normoxic MVs. The RNA coming from normoxic or HR MVs was treated as reported in Fig. 20. The viral DNA showed a drop in the HR MVs mainly after treatment with nucleases which digest the RNA in the R-loops. In normoxic conditions, instead, the drop is visualized mainly before treatment with the Exo S1 nuclease.

The same experiments were conducted on EBV positive MVs and the qPCR products were run on an agarose gel in order to confirm the obtained data. In picture 22 the agarose gel for the EBV, GAPDH and 12S genes amplified after nucleases treatment is reported. The GAPDH gene, found in a dsDNA form since is not eliminated after RNaseH and ExoS1 treatment. The viral and mitochondrial sequences (the 12S gene is known to be characterized by a R-loop structure) are affected by this last treatment. Differences between the GAPDH bands are not evident prior and post DNaseI due to the high number of cycles that we had to perform in order to amplify the viral DNA, which means that its amplification reached the plateau.

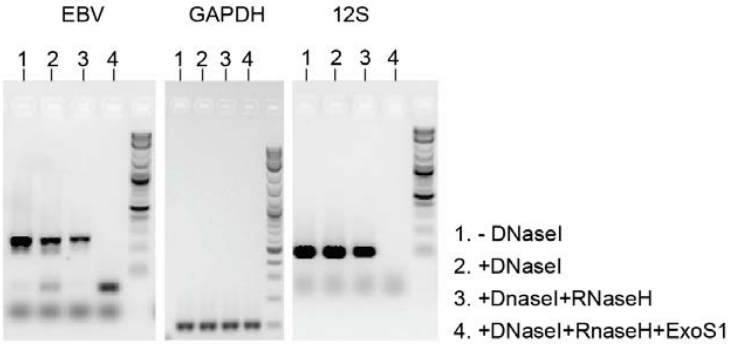

Figure 22: Presence of viral but not nuclear DNA in a R-loop structure in EBV positive HR MVs. DNA from Namalwa MVs was amplified 1) without DNaseI treatment, 2) after DNaseI treatment, 3) after DNAseI and RNaseH treatment and 4) after DNAseI, RNaseH and ExoS1 treatment

In order to confirm the results on the R-loop status of the viral DNA we performed a DNA:RNA immunoprecipitation (DRIP), in which an antibody specific for the DNA:RNA hybrids is used to separate them from the others RNA components. The control of the experiment was characterized by the immunoprecipitation of RNA previously treated with RNAseH, so that in this sample, no DNA amplification should have been determined in the bound fraction.
In figure 23 we report the schematic mechanism of the DRIP assay that takes advantage of an antibody that specifically binds the R-loops called S9.6 Ab.

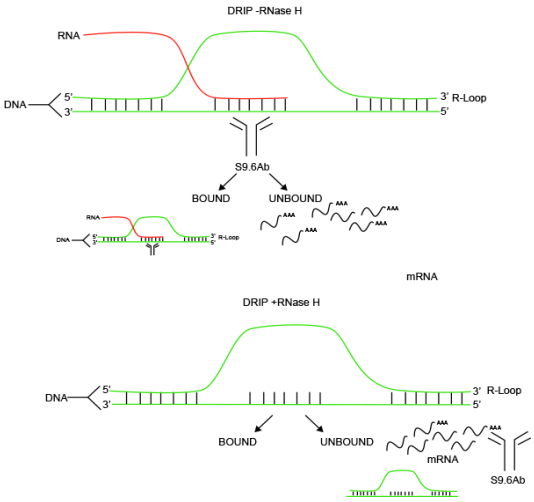

Figure 23: Schematic mechanism of the DRIP assay. Without RNaseH treatment, the Ab can bind the R-loops (bound fraction) discriminating from the other RNA components (unbound fraction). When the RNA is treated with the RNaseH before the DRIP, the RNA molecule in the R-loop is digested; this impedes the Ab to bind the R-loops leading to the presence of the DNA of the DNA:RNA hybrid in the unbound fraction.

In figure 24 we show an agarose gel coming from a DRIP experiment conducted on HR HeLa MVs. Thanks to primers able to amplify both the DNA and the RNA in the same reaction, we were able to identify the viral sequences in the bound and unbound fractions, demonstrating the presence of the R-loops.

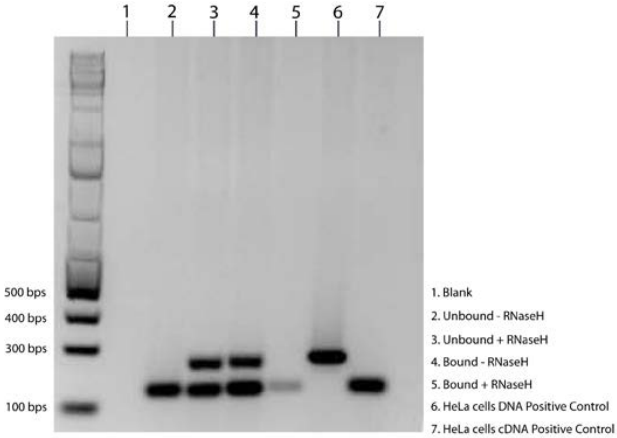

Figure 24: Presence of viral R-loop sequences in HR HeLa MVs by DRIP. When the RNA wasn't treated with the RNAseH, the antibody bound the R-loops, and we were able to amplify both the viral DNA and the RNA (4), while the unbound fraction contained the viral mRNAs only (2); When the RNA was treated with the RNaseH before the DRIP assay, the antibody could no longer bind the R-loops since the RNA molecule was digested. In the unbound fraction we were able to amplify both the viral DNA and RNA (3) while in the bound fraction there was no amplification (5).

By qPCR we were able to calculate the viral RNA copy number of the viral and the difference between the 4 different fractions. As reported in figure 25, in the not RNaseH treated bound fraction, we found an increase of the viral cDNA of almost 80 times compared to the other three fractions.

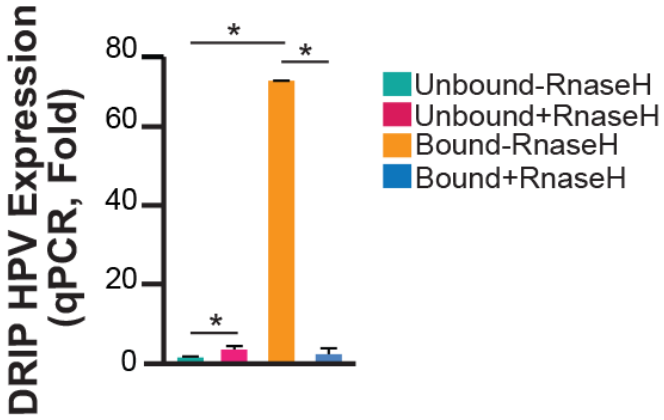

Figure 25: Prevalence of viral RNA in a R-loop form than a mRNA form in HR HeLa MVs. DRIP assay on HR HPV positive MVs. The RNA treated or not treated with RNaseH was dripped and amplified by qPCR for the HPV cDNA. An almost 80 fold increase was determined when the RNA was amplified in the fraction containing the R-loops structures compared to the other fractions.

The presence of complex structures in the microvesicles was finally confirmed by Atomic Force Microscopy (AFM). The nucleic acids coming from HeLa MVs and treated with nucleases were analyzed. In figure 26 we report a picture took by AFM in which is possible to see the difference between the nucleic acids not treated with the nucleases (Panel A) and the ones treated with DNaseI, RNaseH and ExonucleaseS1 (Panel B).

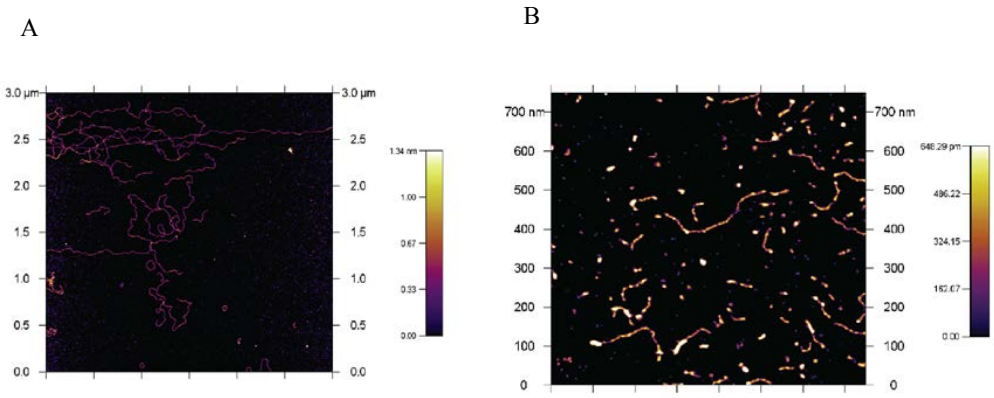

Figure 26: Presence of complex structure in the DNA coming from HR HeLa MVs by Atomic Force Microscopy. (**A**)The DNA not treated with the nucleases is mostly composed by dsDNA, characterized by less thick fragments (purple structures) in the picture. (B) The DNA treated with the DNaseI, RNaseH and ExoS1 is mostly characterized by complex structures which are resistant to the enzymes action and show a higher thickness compared to the linear dsDNA.

Discussion and conclusion

By using cell lines positive for HPV18/16 (Hela/Caski) and EBV (Namalwa) DNA, we were able to isolate microvesides (MVs) positive for viral DNAs. The quality of the microvesicles was tested by electron microscopy and NanoSight analysis. These MVs were used for *in vitro* and *in vivo* experimental studies since they have been either exposed on recipient viral-nucleic acids-negative cells or intravenously injected in breast cancer xenografts. Since the MVs release is different from cells that are cultured in normoxia versus cells grown in hypoxia, we started analyzing if even in our experimental conditions the number of hypoxic MVs was higher than the normoxic ones. After having cultured cells in normoxia or cells that underwent 3 rounds of normoxia and hypoxia treatments, we isolated the MVs and notices that the number of hypoxic MVs was doubled compared to the normoxic ones. We then analyzed the same number of MVs for their DNA concentration and saw a higher concentration in hypoxic/re-oxigenated (HR) MFVs, by Nanodrop. The data was confirmed by qPCR, in which we saw a higher copy number for the nuclear genes (GAPDH, Actin) and the viral oncogenes (HPV16, HPV18 and EBV). MVs Murine cancer associated fibroblasts (mCAFs) were used to study the mitochondrial DNA (mtDNA) transfer: MVs isolated from mCAFs were exposed on human mammary cancer cell lines *in vitro* in order to evaluate the transfer of the mtDNA from one cell to another. After the exposure of the recipient cells to the MVs, we were able to analyze the presence of the viral and mtDNA by PCR and qPCR in the recipient cells in more than one cell line model, but not all. The reason is probably due to the cellular variability and thus, suggests that some cells could be more prone to up take MVs than others. Other than that we visualized, by confocal microscopy, that the time of uptake was different between cancer cells and fibroblasts: the first ones internalized the MVs after about 12 hours while the fibroblasts were positive after only 2 hours post exposure. After the injection of the viral MVs in breast cancer xenografts, we analyzed the presence of the viral DNA (HPV) and RNA (EBV) by colorimetric in situ hybridization (CISH) and were able to identify the nucleic acids in the cancer cells and the surrounding stromal cells. This data was confirmed by creating a Caski xenograft (HPV16 positive cancer cell line): the viral DNA was identified in the stromal compartment also, meaning that the cancer cells produced viral DNA positive MVs that were then up taken by the surrounding stromal cells.

Mitochondrial DNA in the MVs coming from cells that underwent HR treatments was amplified by qPCR and PCR assay. Interestingly, the copy number results showed that mtDNA is enriched in the MVs compared to other nuclear genes (GAPDH) leading to the hypothesis that these microvesicles can actually transfer their content to recipient cells and lead to the development of a heterogeneous environment.

By using primers able to amplify both the DNA and the RNA at the same time (the primers are designed so that they can span the intron between two exons giving rise to two amplicons of different length), we noticed the presence of viral but not nuclear genes in the RNA fraction of viral positive HR MVs (HeLa and Namalwa MVs) even after DNA digestion with DNases treatment (the DNases used in these experiments targeted both the ssDNA and the dsDNA). We then hypothesized that the DNAs that we were able to amplify after nucleases treatment could be protected from the enzyme action and thus, be part of a more complex structure, like an R-loop. In fact, the presence of the resistant DNA was mostly found in HR MVs compared to the normoxic ones and is known that R-loops structures are synthesized more under hypoxic conditions. We thus decided to analyze the status of the viral ad mtDNA in the MVs. After the isolation of the RNA from the viral positive MVs we treated it with different nucleases in order to get rid of the contaminating ss- and dsDNAs; we then treated it with RNases specific for the ss- and ds-RNAs and with a specific RNAse which digests the RNA molecule in the DNA:RNA hybrid. After all these steps we performed PCRs and still we were able to amplify the viral sequences. Only after a last step in

which we repeated the treatment with a ssDNA specific DNase, we were no longer able to visualize the viral DNA, leading to the conclusion that the viral DNA was effectively part of the DNA:RNA hybrid structure. Since R-Loops are known to be really stable structures, we hypothesized that the viral DNA could be incorporated in these complexes and be more protected from cellular degradation once the MVs get in the recipient cells. To verify these results, we performed a DNA/RNA immunoprecipitation (DRIP) using a specific antibody, which recognizes the R-loop structure, in the RNA coming from HeLa HR MVs and looked for the presence of both genomic and viral DNA in the bound and unbound fractions. Thanks to a copy number analysis, we were able to identify a fold increase of 80 times of the viral DNA sequence in the bound (R-loop enriched) fraction compare to the unbound fraction.

After having conducted all these experiments in vitro, we decided to analyze the presence of viral and mitochondrial DNA in circulating MVs coming from newly diagnosed breast cancer patients, collected by the Sant' Orsola-Malpighi Hospital, located in Bologna, Italy, and patients affected by hormonal therapy resistant breast cancer, collected by the Memorial Sloan Kettering Cancer Center (MSKCC), located in New York, USA. Analyzing the Italian cohort, we were able to identify HPV DNA sequences in the 11% (8/68) of the samples by PCR; the 4% of the samples tested positive to the HPV16 (3/68), the 6% to the HPV18 DNA (4/68) and the 1% to the HPV31. In the American cohort we were able to screen the viral, nuclear and mtDNA and calculate their copy number. The data showed a total positivity of the 14% to the viral DNAs (9/65); HPV16 was found in the 6% (4/65) of the samples, the HPV18 in the 5% (3/65) and the 3% of the samples (2/65) showed the presence of a HPV16/18 co-infection. The presence of the mitochondrial DNA was evaluated and found in the 72% of the specimens compared to a 37% of positivity to the GAPDH gene. This results lead to hypothesize that nuclear, viral and mitochondrial DNAs are probably released in different ways and amounts depending on the cells releasing them and the pathological conditions of the patients.

Finally, the complex nucleic acids structures obtained after nucleases treatments were visualized by atomic force microscopy. In particular, we compared the DNA not treated with nucleases or treated with DNaseI, RNaseH and ExonucleaseS1, coming from HPV and EBV DNA positive HR MVs. By AFM we could see how the not treated fraction was mainly characterized by dsDNAs while the treated one mainly showed the presence of structures with a higher color density, which correlates with a higher structure complexity.

Thanks to these experiments, we were able to determine a possible mechanism of viral nucleic acids transfer from a primary site of infection to different not permissive tissues, through microvesicles together with their chemical-physical status. We were able to verify a possible mechanism of mitochondrial DNA transfer from one cell to another, opening the possibility of a different acquisition of foreign material through microvesicles, in a neoplastic environment. We identified viral DNA sequences in circulating MVs of breast cancer patients either newly diagnosed or affected by a hormonal therapy resistant disease and we also demonstrated a high presence of mtDNA in the microvesicles in the American cohort.

Taken together, these data demonstrate how microvesicles can play a role in the tumor heterogeneity development. Further studies will be conducted in order to evaluate a possible correlation between the presence of the viral and mtDNA in MVs and development of an aggressive tumor phenotype in breast cancer patients, analyzing the mtDNA also in the MVs of newly diagnosed breast cancer patients and comparing it to the MVs of patients with an HTR disease; also further investigation will be conducted to understand if the viral and mitochondrial nucleic acids transferred by microvesicles can be responsible for metastatic progression and resistance to therapies in luminal breast cancer models.

Bibliography

Adey A, Burton JN, Kitzman JO, Hiatt JB, Lewis AP, et al. The haplotype-resolved genome and epigenome of the aneuploid HeLa cancer cell line. Nature. 2013 Aug 8;500(7461):207-11. PubMed PMID: 23925245; NIHMSID: NIHMS454925; PubMed Central PMCID: PMC3740412.

Al-Nedawi K, Meehan B, Micallef J, Lhotak V, May L, et al. Intercellular transfer of the oncogenic receptor EGFRvIII by microvesicles derived from tumour cells. Nat Cell Biol. 2008 May;10(5):619-24. PubMed PMID: 18425114.

Anderson S, Bankier AT, Barrell BG, de Bruijn MH, Coulson AR, et al. Sequence and organization of the human mitochondrial genome. Nature. 1981 Apr 9;290(5806):457-65. PubMed PMID: 7219534.

Andreola G, Rivoltini L, Castelli C, Huber V, Perego P, et al. Induction of lymphocyte apoptosis by tumor cell secretion of FasL-bearing microvesicles. J Exp Med. 2002 May 20;195(10):1303-16. PubMed PMID: 12021310; PubMed Central PMCID: PMC2193755.

Angelucci A, D'Ascenzo S, Festuccia C, Gravina GL, Bologna M, et al. Vesicle-associated urokinase plasminogen activator promotes invasion in prostate cancer cell lines. Clin Exp Metastasis. 2000;18(2):163-70. PubMed PMID: 11235992.

Bainton DF. The discovery of lysosomes. J Cell Biol. 1981 Dec;91(3 Pt 2):66s-76s. PubMed PMID: 7033245; PubMed Central PMCID: PMC2112804.

Baj-Krzyworzeka M, Szatanek R, Weglarczyk K, Baran J, Urbanowicz B, et al. Tumour-derived microvesicles carry several surface determinants and mRNA of tumour cells and transfer some of these determinants to monocytes. Cancer Immunol Immunother. 2006 Jul;55(7):808-18. PubMed PMID: 16283305.

Bajetta E, Zilembo N, Bichisao E, Martinetti A, Buzzoni R, et al. Tumor response and estrogen suppression in breast cancer patients treated with aromatase inhibitors. Ann Oncol. 2000 Aug;11(8):1017-22. PubMed PMID: 11038039.

Balaj L, Lessard R, Dai L, Cho YJ, Pomeroy SL, et al. Tumour microvesicles contain retrotransposon elements and amplified oncogene sequences. Nat Commun. 2011 Feb 1;2:180. PubMed PMID: 21285958; NIHMSID: NIHMS270621; PubMed Central PMCID: PMC3040683.

Bhatia V, Barroso SI, García-Rubio ML, Tumini E, Herrera-Moyano E, et al. BRCA2 prevents R-loop accumulation and associates with TREX-2 mRNA export factor PCID2. Nature. 2014 Jul 17;511(7509):362-5. PubMed PMID: 24896180.

Bonnet M, Guinebretiere JM, Kremmer E, Grunewald V, Benhamou E, et al. Detection of Epstein-Barr virus in invasive breast cancers. J Natl Cancer Inst. 1999 Aug 18;91(16):1376-81. PubMed PMID: 10451442.

Boshart M, Gissmann L, Ikenberg H, Kleinheinz A, Scheurlen W, et al. A new type of papillomavirus DNA, its presence in genital cancer biopsies and in cell lines derived from cervical cancer. EMBO J. 1984 May;3(5):1151-7. PubMed PMID: 6329740; PubMed Central PMCID: PMC557488.

Brandon M, Baldi P, Wallace DC. Mitochondrial mutations in cancer. Oncogene. 2006 Aug 7;25(34):4647-62. PubMed PMID: 16892079.

Castellana D, Zobairi F, Martinez MC, Panaro MA, Mitolo V, et al. Membrane microvesicles as actors in the establishment of a favorable prostatic tumoral niche: a role for activated fibroblasts and CX3CL1-CX3CR1 axis. Cancer Res. 2009 Feb 1;69(3):785-93. PubMed PMID: 19155311.

Castellano-Pozo M, Santos-Pereira JM, Rondón AG, Barroso S, Andújar E, et al. R loops are linked to histone H3 S10 phosphorylation and chromatin condensation. Mol Cell. 2013 Nov 21;52(4):583-90. PubMed PMID: 24211264.

Charras GT, Yarrow JC, Horton MA, Mahadevan L, Mitchison TJ. Non-equilibration of hydrostatic pressure in blebbing cells. Nature. 2005 May 19;435(7040):365-9. PubMed PMID: 15902261; NIHMSID: NIHMS4384; PubMed Central PMCID: PMC1564437.

Chen X, Ba Y, Ma L, Cai X, Yin Y, et al. Characterization of microRNAs in serum: a novel class of biomarkers for diagnosis of cancer and other diseases. Cell Res. 2008 Oct;18(10):997-1006. PubMed PMID: 18766170.

Chen YC, Chen JH, Richard K, Chen PY, Christiani DC. Lung adenocarcinoma and human papillomavirus infection. Cancer. 2004 Sep 15;101(6):1428-36. PubMed PMID: 15368331.

Chomyn A, Mariottini P, Cleeter MW, Ragan CI, Matsuno-Yagi A, et al. Six unidentified reading frames of human mitochondrial DNA encode components of the respiratory-chain NADH dehydrogenase. Nature. 1985 Apr 18-24;314(6012):592-7. PubMed PMID: 3921850.

Chong T, Apt D, Gloss B, Isa M, Bernard HU. The enhancer of human papillomavirus type 16: binding sites for the ubiquitous transcription factors oct-1, NFA, TEF-2, NF1, and AP-1 participate in epithelial cell-specific transcription. J Virol. 1991 Nov;65(11):5933-43. PubMed PMID: 1656080; PubMed Central PMCID: PMC250257.

Cocucci E, Racchetti G, Meldolesi J. Shedding microvesicles: artefacts no more. Trends Cell Biol. 2009 Feb;19(2):43-51. PubMed PMID: 19144520.

Dames S, Eilbeck K, Mao R. A high-throughput next-generation sequencing assay for the mitochondrial genome. Methods Mol Biol. 2015;1264:77-88. PubMed PMID: 25631005.

Daniels GA, Lieber MR. RNA:DNA complex formation upon transcription of immunoglobulin switch regions: implications for the mechanism and regulation of class switch recombination. Nucleic Acids Res. 1995 Dec 25;23(24):5006-11. PubMed PMID: 8559658; PubMed Central PMCID: PMC307506.

de Bruijn WC. Glycogen, its chemistry and morphologic appearance in the electron microscope I A modified OsO 4 fixative which selectively contrasts glycogen. J Ultrastruct Res. 1973 Jan;42(1):29-50. PubMed PMID: 4567407.

de Villiers EM, Fauquet C, Broker TR, Bernard HU, zur Hausen H. Classification of papillomaviruses. Virology. 2004 Jun 20;324(1):17-27. PubMed PMID: 15183049.

Del Conde I, Shrimpton CN, Thiagarajan P, López JA. Tissue-factor-bearing microvesicles arise from lipid rafts and fuse with activated platelets to initiate coagulation. Blood. 2005 Sep 1;106(5):1604-11. PubMed PMID: 15741221.

Di Lonardo A, Venuti A, Marcante ML. Human papillomavirus in breast cancer. Breast Cancer Res Treat. 1992;21(2):95-100. PubMed PMID: 1320958.

Di Vizio D, Kim J, Hager MH, Morello M, Yang W, et al. Oncosome formation in prostate cancer: association with a region of frequent chromosomal deletion in metastatic disease. Cancer Res. 2009 Jul 1;69(13):5601-9. PubMed PMID: 19549916; NIHMSID: NIHMS115499; PubMed Central PMCID: PMC2853876.

Dolo V, Ginestra A, Cassarà D, Violini S, Lucania G, et al. Selective localization of matrix metalloproteinase 9, beta1 integrins, and human lymphocyte antigen class I molecules on membrane vesicles shed by 8701-BC breast carcinoma cells. Cancer Res. 1998 Oct 1;58(19):4468-74. PubMed PMID: 9766680.

Doorbar J, Egawa N, Griffin H, Kranjec C, Murakami I. Human papillomavirus molecular biology and disease association. Rev Med Virol. 2015 Mar;25 Suppl 1:2-23. PubMed PMID: 25752814.

Drolet M, Bi X, Liu LF. Hypernegative supercoiling of the DNA template during transcription elongation in vitro. J Biol Chem. 1994 Jan 21;269(3):2068-74. PubMed PMID: 8294458.

Eliopoulos AG, Stack M, Dawson CW, Kaye KM, Hodgkin L, et al. Epstein-Barr virus-encoded LMP1 and CD40 mediate IL-6 production in epithelial cells via an NF-kappaB pathway involving TNF receptor-associated factors. Oncogene. 1997 Jun 19;14(24):2899-916. PubMed PMID: 9205097.

Eliopoulos AG, Gallagher NJ, Blake SM, Dawson CW, Young LS. Activation of the p38 mitogen-activated protein kinase pathway by Epstein-Barr virus-encoded latent membrane protein 1 coregulates interleukin-6 and interleukin-8 production. J Biol Chem. 1999 Jun 4;274(23):16085-96. PubMed PMID: 10347160.

Epstein MA, Achong BG, Barr YM. Virus particles in cultured lymphoblasts from Burkitt's Lymhoma. Lancet. 1964 Mar 28;1(7335):702-3. PubMed PMID: 14107961.

Falchi AM, Sogos V, Saba F, Piras M, Congiu T, et al. Astrocytes shed large membrane vesicles that contain mitochondria, lipid droplets and ATP. Histochem Cell Biol. 2013 Feb;139(2):221-31. PubMed PMID: 23108569.

Fidler IJ. The pathogenesis of cancer metastasis: the 'seed and soil' hypothesis revisited. Nat Rev Cancer. 2003 Jun;3(6):453-8. PubMed PMID: 12778135.

Flanagan J, Middeldorp J, Sculley T. Localization of the Epstein-Barr virus protein LMP 1 to exosomes. J Gen Virol. 2003 Jul;84(Pt 7):1871-9. PubMed PMID: 12810882.

Friend C, Marovitz W, Henie G, Henie W, Tsuei D, et al. Observations on cell lines derived from a patient with Hodgkin's disease. Cancer Res. 1978 Aug;38(8):2581-91. PubMed PMID: 78764.

Gaiffe E, Prétet JL, Launay S, Jacquin E, Saunier M, et al. Apoptotic HPV positive cancer cells exhibit transforming properties. PLoS One. 2012;7(5):e36766. PubMed PMID: 22574222; PubMed Central PMCID: PMC3344932.

Giacinti C, Giordano A. RB and cell cycle progression. Oncogene. 2006 Aug 28;25(38):5220-7. PubMed PMID: 16936740.

Ginestra A, La Placa MD, Saladino F, Cassarà D, Nagase H, et al. The amount and proteolytic content of vesicles shed by human cancer cell lines correlates with their in vitro invasiveness. Anticancer Res. 1998 Sep-Oct;18(5A):3433-7. PubMed PMID: 9858920.

Ginno PA, Lott PL, Christensen HC, Korf I, Chédin F. R-loop formation is a distinctive characteristic of unmethylated human CpG island promoters. Mol Cell. 2012 Mar 30;45(6):814-25. PubMed PMID: 22387027; NIHMSID: NIHMS362480; PubMed Central PMCID: PMC3319272.

Giusti I, D'Ascenzo S, Millimaggi D, Taraboletti G, Carta G, et al. Cathepsin B mediates the pH-dependent proinvasive activity of tumor-shed microvesicles. Neoplasia. 2008 May;10(5):481-8. PubMed PMID: 18472965; PubMed Central PMCID: PMC2373913.

Graves LE, Ariztia EV, Navari JR, Matzel HJ, Stack MS, et al. Proinvasive properties of ovarian cancer ascites-derived membrane vesicles. Cancer Res. 2004 Oct 1;64(19):7045-9. PubMed PMID: 15466198.

Grossman SR, Johannsen E, Tong X, Yalamanchili R, Kieff E. The Epstein-Barr virus nuclear antigen 2 transactivator is directed to response elements by the J kappa recombination signal binding protein. Proc Natl Acad Sci U S A. 1994 Aug 2;91(16):7568-72. PubMed PMID: 8052621; PubMed Central PMCID: PMC44443.

Guescini M, Guidolin D, Vallorani L, Casadei L, Gioacchini AM, et al. C2C12 myoblasts release micro-vesicles containing mtDNA and proteins involved in signal transduction. Exp Cell Res. 2010 Jul 15;316(12):1977-84. PubMed PMID: 20399774.

Gulley ML, Pulitzer DR, Eagan PA, Schneider BG. Epstein-Barr virus infection is an early event in gastric carcinogenesis and is independent of bcl-2 expression and p53 accumulation. Hum Pathol. 1996 Jan;27(1):20-7. PubMed PMID: 8543306.

Gutensohn N, Cole P. Epidemiology of Hodgkin's disease. Semin Oncol. 1980 Jun;7(2):92-102. PubMed PMID: 6255608.

Hakulinen J, Sankkila L, Sugiyama N, Lehti K, Keski-Oja J. Secretion of active membrane type 1 matrix metalloproteinase (MMP-14) into extracellular space in microvesicular exosomes. J Cell Biochem. 2008 Dec 1;105(5):1211-8. PubMed PMID: 18802920.

Hammerschmidt W, Sugden B. Genetic analysis of immortalizing functions of Epstein-Barr virus in human B lymphocytes. Nature. 1989 Aug 3;340(6232):393-7. PubMed PMID: 2547164.

Helmrich A, Ballarino M, Tora L. Collisions between replication and transcription complexes cause common fragile site instability at the longest human genes. Mol Cell. 2011 Dec 23;44(6):966-77. PubMed PMID: 22195969.

Henderson S, Rowe M, Gregory C, Croom-Carter D, Wang F, et al. Induction of bcl-2 expression by Epstein-Barr virus latent membrane protein 1 protects infected B cells from programmed cell death. Cell. 1991 Jun 28;65(7):1107-15. PubMed PMID: 1648447.

Heng B, Glenn WK, Ye Y, Tran B, Delprado W, et al. Human papilloma virus is associated with breast cancer. Br J Cancer. 2009 Oct 20;101(8):1345-50. PubMed PMID: 19724278; PubMed Central PMCID: PMC2737128.

Henle G, Henle W. Epstein-Barr virus-specific IgA serum antibodies as an outstanding feature of nasopharyngeal carcinoma. Int J Cancer. 1976 Jan 15;17(1):1-7. PubMed PMID: 175020.

Herrmann K, Niedobitek G. Epstein-Barr virus-associated carcinomas: facts and fiction. J Pathol. 2003 Feb;199(2):140-5. PubMed PMID: 12533825.

Hotary K, Li XY, Allen E, Stevens SL, Weiss SJ. A cancer cell metalloprotease triad regulates the basement membrane transmigration program. Genes Dev. 2006 Oct 1;20(19):2673-86. PubMed PMID: 16983145; PubMed Central PMCID: PMC1578694.

Huber V, Fais S, Iero M, Lugini L, Canese P, et al. Human colorectal cancer cells induce T-cell death through release of proapoptotic microvesicles: role in immune escape. Gastroenterology. 2005 Jun;128(7):1796-804. PubMed PMID: 15940614.

Huertas P, Aguilera A. Cotranscriptionally formed DNA:RNA hybrids mediate transcription elongation impairment and transcription-associated recombination. Mol Cell. 2003 Sep;12(3):711-21. PubMed PMID: 14527416.

Huo Q, Zhang N, Yang Q. Epstein-Barr virus infection and sporadic breast cancer risk: a meta-analysis. PLoS One. 2012;7(2):e31656. PubMed PMID: 22363698; PubMed Central PMCID: PMC3283657.

Iero M, Valenti R, Huber V, Filipazzi P, Parmiani G, et al. Tumour-released exosomes and their implications in cancer immunity. Cell Death Differ. 2008 Jan;15(1):80-8. PubMed PMID: 17932500.

Kajitani N, Satsuka A, Kawate A, Sakai H. Productive Lifecycle of Human Papillomaviruses that Depends Upon Squamous Epithelial Differentiation. Front Microbiol. 2012;3:152. PubMed PMID: 22536200; PubMed Central PMCID: PMC3334820.

Kim CW, Lee HM, Lee TH, Kang C, Kleinman HK, et al. Extracellular membrane vesicles from tumor cells promote angiogenesis via sphingomyelin. Cancer Res. 2002 Nov 1;62(21):6312-7. PubMed PMID: 12414662.

Kim JW, Wieckowski E, Taylor DD, Reichert TE, Watkins S, et al. Fas ligand-positive membranous vesicles isolated from sera of patients with oral cancer induce apoptosis of activated T lymphocytes. Clin Cancer Res. 2005 Feb 1;11(3):1010-20. PubMed PMID: 15709166.

Labrecque LG, Barnes DM, Fentiman IS, Griffin BE. Epstein-Barr virus in epithelial cell tumors: a breast cancer study. Cancer Res. 1995 Jan 1;55(1):39-45. PubMed PMID: 7805038.

Laherty CD, Hu HM, Opipari AW, Wang F, Dixit VM. The Epstein-Barr virus LMP1 gene product induces A20 zinc finger protein expression by activating nuclear factor kappa B. J Biol Chem. 1992 Dec 5;267(34):24157-60. PubMed PMID: 1332946.

Lawrie CH, Gal S, Dunlop HM, Pushkaran B, Liggins AP, et al. Detection of elevated levels of tumour-associated microRNAs in serum of patients with diffuse large B-cell lymphoma. Br J Haematol. 2008 May;141(5):672-5. PubMed PMID: 18318758.

Leone G, Larocca LM, Pizzigallo E. Introducing mediterranean journal of hematology and infectious diseases. Mediterr J Hematol Infect Dis. 2009 Jun 17;1(1):e2009001. PubMed PMID: 21415983; PubMed Central PMCID: PMC3033169.

Lie AK, Kristensen G. Human papillomavirus E6/E7 mRNA testing as a predictive marker for cervical carcinoma. Expert Rev Mol Diagn. 2008 Jul;8(4):405-15. PubMed PMID: 18598223.

Mack M, Kleinschmidt A, Brühl H, Klier C, Nelson PJ, et al. Transfer of the chemokine receptor CCR5 between cells by membrane-derived microparticles: a mechanism for cellular human immunodeficiency virus 1 infection. Nat Med. 2000 Jul;6(7):769-75. PubMed PMID: 10888925.

Macreadie IG, Novitski CE, Maxwell RJ, John U, Ooi BG, et al. Biogenesis of mitochondria: the mitochondrial gene (aap1) coding for mitochondrial ATPase subunit 8 in Saccharomyces cerevisiae. Nucleic Acids Res. 1983 Jul 11;11(13):4435-51. PubMed PMID: 6223276; PubMed Central PMCID: PMC326057.

Mazouni C, Fina F, Romain S, Ouafik L, Bonnier P, et al. Epstein-Barr virus as a marker of biological aggressiveness in breast cancer. Br J Cancer. 2011 Jan 18;104(2):332-7. PubMed PMID: 21179039; PubMed Central PMCID: PMC3031896.

McConnell RE, Higginbotham JN, Shifrin DA Jr, Tabb DL, Coffey RJ, et al. The enterocyte microvillus is a vesicle-generating organelle. J Cell Biol. 2009 Jun 29;185(7):1285-98. PubMed PMID: 19564407; PubMed Central PMCID: PMC2712962.

McKinney EA, Oliveira MT. Replicating animal mitochondrial DNA. Genet Mol Biol. 2013 Sep;36(3):308-15. PubMed PMID: 24130435; PubMed Central PMCID: PMC3795181.

Meckes DG Jr, Raab-Traub N. Microvesicles and viral infection. J Virol. 2011 Dec;85(24):12844-54. PubMed PMID: 21976651; PubMed Central PMCID: PMC3233125.

Miller G. The oncogenicity of Epstein-Barr virus. J Infect Dis. 1974 Aug;130(2):187-205. PubMed PMID: 4366977.

Millimaggi D, Mari M, D'Ascenzo S, Carosa E, Jannini EA, et al. Tumor vesicle-associated CD147 modulates the angiogenic capability of endothelial cells. Neoplasia. 2007 Apr;9(4):349-57. PubMed PMID: 17460779; PubMed Central PMCID: PMC1854851.

Milsom C, Yu J, May L, Meehan B, Magnus N, et al. The role of tumor-and host-related tissue factor pools in oncogene-driven tumor progression. Thromb Res. 2007;120 Suppl 2:S82-91. PubMed PMID: 18023719.

Mitchell PS, Parkin RK, Kroh EM, Fritz BR, Wyman SK, et al. Circulating microRNAs as stable blood-based markers for cancer detection. Proc Natl Acad Sci U S A. 2008 Jul 29;105(30):10513-8. PubMed PMID: 18663219; PubMed Central PMCID: PMC2492472.

Möbius W, van Donselaar E, Ohno-Iwashita Y, Shimada Y, Heijnen HF, et al. Recycling compartments and the internal vesicles of multivesicular bodies harbor most of the cholesterol found in the endocytic pathway. Traffic. 2003 Apr;4(4):222-31. PubMed PMID: 12694561.

Muralidharan-Chari V, Clancy JW, Sedgwick A, D'Souza-Schorey C. Microvesicles: mediators of extracellular communication during cancer progression. J Cell Sci. 2010 May 15;123(Pt 10):1603-11. PubMed PMID: 20445011; PubMed Central PMCID: PMC2864708.

Muralidharan-Chari V, Clancy J, Plou C, Romao M, Chavrier P, et al. ARF6-regulated shedding of tumor cell-derived plasma membrane microvesicles. Curr Biol. 2009 Dec 1;19(22):1875-85. PubMed PMID: 19896381; NIHMSID: NIHMS150848; PubMed Central PMCID: PMC3150487.

Nakama M, Kawakami K, Kajitani T, Urano T, Murakami Y. DNA-RNA hybrid formation mediates RNAi-directed heterochromatin formation. Genes Cells. 2012 Mar;17(3):218-33. PubMed PMID: 22280061.

Odumade OA, Hogquist KA, Balfour HH Jr. Progress and problems in understanding and managing primary Epstein-Barr virus infections. Clin Microbiol Rev. 2011 Jan;24(1):193-209. PubMed PMID: 21233512; PubMed Central PMCID: PMC3021204.

Paluch E, Piel M, Prost J, Bornens M, Sykes C. Cortical actomyosin breakage triggers shape oscillations in cells and cell fragments. Biophys J. 2005 Jul;89(1):724-33. PubMed PMID: 15879479; PubMed Central PMCID: PMC1366569.

Pegtel DM, Cosmopoulos K, Thorley-Lawson DA, van Eijndhoven MA, Hopmans ES, et al. Functional delivery of viral miRNAs via exosomes. Proc Natl Acad Sci U S A. 2010 Apr 6;107(14):6328-33. PubMed PMID: 20304794; PubMed Central PMCID: PMC2851954.

Piccin A, Murphy WG, Smith OP. Circulating microparticles: pathophysiology and clinical implications. Blood Rev. 2007 May;21(3):157-71. PubMed PMID: 17118501.

Pioche-Durieu C, Keryer C, Souquère S, Bosq J, Faigle W, et al. In nasopharyngeal carcinoma cells, Epstein-Barr virus LMP1 interacts with galectin 9 in membrane raft elements resistant to simvastatin. J Virol. 2005 Nov;79(21):13326-37. PubMed PMID: 16227255; PubMed Central PMCID: PMC1262583.

Pope JH, Achong BG, Epstein MA. Cultivation and fine structure of virus-bearing lymphoblasts from a second New Guinea Burkitt lymphoma: establishment of sublines with unusual cultural properties. Int J Cancer. 1968 Mar 15;3(2):171-82. PubMed PMID: 5649156.

Rak J. Microparticles in cancer. Semin Thromb Hemost. 2010 Nov;36(8):888-906. PubMed PMID: 21049390.

Rana A, Rangasamy V, Mishra R. How estrogen fuels breast cancer. Future Oncol. 2010 Sep;6(9):1369-71. PubMed PMID: 20919821.

Rappa G, Mercapide J, Anzanello F, Pope RM, Lorico A. Biochemical and biological characterization of exosomes containing prominin-1/CD133. Mol Cancer. 2013 Jun 14;12:62. PubMed PMID: 23767874; PubMed Central PMCID: PMC3698112.

Ratajczak J, Wysoczynski M, Hayek F, Janowska-Wieczorek A, Ratajczak MZ. Membrane-derived microvesicles: important and underappreciated mediators of cell-to-cell communication. Leukemia. 2006 Sep;20(9):1487-95. PubMed PMID: 16791265.

Ratajczak J, Miekus K, Kucia M, Zhang J, Reca R, et al. Embryonic stem cell-derived microvesicles reprogram hematopoietic progenitors: evidence for horizontal transfer of mRNA and protein delivery. Leukemia. 2006 May;20(5):847-56. PubMed PMID: 16453000.

Rickinson AB, Rowe M, Hart IJ, Yao QY, Henderson LE, et al. T-cell-mediated regression of "spontaneous" and of Epstein-Barr virus-induced B-cell transformation in vitro: studies with cyclosporin A. Cell Immunol. 1984 Sep;87(2):646-58. PubMed PMID: 6088089.

Rous P. A Sarcoma of the fowl transmissible by an agent separable from the tumor cells. J Exp Med. 1911 Apr 1;13(4):397-411. PubMed PMID: 19867421; PubMed Central PMCID: PMC2124874.

Rowe M, Peng-Pilon M, Huen DS, Hardy R, Croom-Carter D, et al. Upregulation of bcl-2 by the Epstein-Barr virus latent membrane protein LMP1: a B-cell-specific response that is delayed relative to NF-kappa B activation and to induction of cell surface markers. J Virol. 1994 Sep;68(9):5602-12. PubMed PMID: 7520093; PubMed Central PMCID: PMC236961.

Sanderson MP, Keller S, Alonso A, Riedle S, Dempsey PJ, et al. Generation of novel, secreted epidermal growth factor receptor (EGFR/ErbB1) isoforms via metalloprotease-dependent ectodomain shedding and exosome secretion. J Cell Biochem. 2008 Apr 15;103(6):1783-97. PubMed PMID: 17910038.

Santos-Pereira JM, Herrero AB, García-Rubio ML, Marín A, Moreno S, et al. The Npl3 hnRNP prevents R-loop-mediated transcription-replication conflicts and genome instability. Genes Dev. 2013 Nov 15;27(22):2445-58. PubMed PMID: 24240235; PubMed Central PMCID: PMC3841734.

Schneider-Maunoury S. [Papillomaviruses and cancer]. Rev Prat. 1987 Oct 22;37(42):2567-72. PubMed PMID: 2827294.

Scott CC, Vacca F, Gruenberg J. Endosome maturation, transport and functions. Semin Cell Dev Biol. 2014 Jul;31:2-10. PubMed PMID: 24709024.

Sidhu SS, Mengistab AT, Tauscher AN, LaVail J, Basbaum C. The microvesicle as a vehicle for EMMPRIN in tumor-stromal interactions. Oncogene. 2004 Jan 29;23(4):956-63. PubMed PMID: 14749763.

Simões PW, Medeiros LR, Simões Pires PD, Edelweiss MI, Rosa DD, et al. Prevalence of human papillomavirus in breast cancer: a systematic review. Int J Gynecol Cancer. 2012 Mar;22(3):343-7. PubMed PMID: 22214962.

Skog J, Würdinger T, van Rijn S, Meijer DH, Gainche L, et al. Glioblastoma microvesicles transport RNA and proteins that promote tumour growth and provide diagnostic biomarkers. Nat Cell Biol. 2008 Dec;10(12):1470-6. PubMed PMID: 19011622; NIHMSID: NIHMS70106; PubMed Central PMCID: PMC3423894.

Smalley DM, Sheman NE, Nelson K, Theodorescu D. Isolation and identification of potential urinary microparticle biomarkers of bladder cancer. J Proteome Res. 2008 May;7(5):2088-96. PubMed PMID: 18373357.

Sollier J, Cimprich KA. Breaking bad: R-loops and genome integrity. Trends Cell Biol. 2015 Sep;25(9):514-22. PubMed PMID: 26045257; NIHMSID: NIHMS690810; PubMed Central PMCID: PMC4554970.

Sordet O, Redon CE, Guirouilh-Barbat J, Smith S, Solier S, et al. Ataxia telangiectasia mutated activation by transcription- and topoisomerase I-induced DNA double-strand breaks. EMBO Rep. 2009 Aug;10(8):887-93. PubMed PMID: 19557000; PubMed Central PMCID: PMC2726680.

Sørlie T. Molecular portraits of breast cancer: tumour subtypes as distinct disease entities. Eur J Cancer. 2004 Dec;40(18):2667-75. PubMed PMID: 15571950.

Stubenrauch F, Laimins LA. Human papillomavirus life cycle: active and latent phases. Semin Cancer Biol. 1999 Dec;9(6):379-86. PubMed PMID: 10712884.

Taher C, de Boniface J, Mohammad AA, Religa P, Hartman J, et al. High prevalence of human cytomegalovirus proteins and nucleic acids in primary breast cancer and metastatic sentinel lymph nodes. PLoS One. 2013;8(2):e56795. PubMed PMID: 23451089; PubMed Central PMCID: PMC3579924.

Taraboletti G, D'Ascenzo S, Giusti I, Marchetti D, Borsotti P, et al. Bioavailability of VEGF in tumor-shed vesicles depends on vesicle burst induced by acidic pH. Neoplasia. 2006 Feb;8(2):96-103. PubMed PMID: 16611402; PubMed Central PMCID: PMC1578512.

Taylor DD, Gercel-Taylor C. MicroRNA signatures of tumor-derived exosomes as diagnostic biomarkers of ovarian cancer. Gynecol Oncol. 2008 Jul;110(1):13-21. PubMed PMID: 18589210.

Tesselaar ME, Romijn FP, Van Der Linden IK, Prins FA, Bertina RM, et al. Microparticle-associated tissue factor activity: a link between cancer and thrombosis?. J Thromb Haemost. 2007 Mar;5(3):520-7. PubMed PMID: 17166244.

Thakur BK, Zhang H, Becker A, Matei I, Huang Y, et al. Double-stranded DNA in exosomes: a novel biomarker in cancer detection. Cell Res. 2014 Jun;24(6):766-9. PubMed PMID: 24710597; PubMed Central PMCID: PMC4042169.

Théry C, Regnault A, Garin J, Wolfers J, Zitvogel L, et al. Molecular characterization of dendritic cell-derived exosomes Selective accumulation of the heat shock protein hsc73. J Cell Biol. 1999 Nov 1;147(3):599-610. PubMed PMID: 10545503; PubMed Central PMCID: PMC2151184.

Thomas M, White RL, Davis RW. Hybridization of RNA to double-stranded DNA: formation of R-loops. Proc Natl Acad Sci U S A. 1976 Jul;73(7):2294-8. PubMed PMID: 781674; PubMed Central PMCID: PMC430535.

Trams EG, Lauter CJ, Salem N Jr, Heine U. Exfoliation of membrane ecto-enzymes in the form of micro-vesicles. Biochim Biophys Acta. 1981 Jul 6;645(1):63-70. PubMed PMID: 6266476.

Venhable JH, Coggeshall R. A Simplified lead citrate stain for use in electron microscopy. J Cell Biol. 1965 May;25:407-8. PubMed PMID: 14287192; PubMed Central PMCID: PMC2106628.

Vidone M, Alessandrini F, Marucci G, Farnedi A, de Biase D, et al. Evidence of association of human papillomavirus with prognosis worsening in glioblastoma multiforme. Neuro Oncol. 2014 Jan;16(2):298-302. PubMed PMID: 24285549; PubMed Central PMCID: PMC3895373.

Widschwendter A, Brunhuber T, Wiedemair A, Mueller-Holzner E, Marth C. Detection of human papillomavirus DNA in breast cancer of patients with cervical cancer history. J Clin Virol. 2004 Dec;31(4):292-7. PubMed PMID: 15494272.

Wongsurawat T, Jenjaroenpun P, Kwoh CK, Kuznetsov V. Quantitative model of R-loop forming structures reveals a novel level of RNA-DNA interactome complexity. Nucleic Acids Res. 2012 Jan;40(2):e16. PubMed PMID: 22121227; PubMed Central PMCID: PMC3258121.

Xu B, Clayton DA. RNA-DNA hybrid formation at the human mitochondrial heavy-strand origin ceases at replication start sites: an implication for RNA-DNA hybrids serving as primers. EMBO J. 1996 Jun 17;15(12):3135-43. PubMed PMID: 8670814; PubMed Central PMCID: PMC450256.

Yang Y, McBride KM, Hensley S, Lu Y, Chedin F, et al. Arginine methylation facilitates the recruitment of TOP3B to chromatin to prevent R loop accumulation. Mol Cell. 2014 Feb 6;53(3):484-97. PubMed PMID: 24507716; NIHMSID: NIHMS562215; PubMed Central PMCID: PMC3959860.

Young LS, Dawson CW, Eliopoulos AG. Epstein-Barr virus and apoptosis: viral mimicry of cellular pathways. Biochem Soc Trans. 1999 Dec;27(6):807-12. PubMed PMID: 10830106.

Young LS, Rickinson AB. Epstein-Barr virus: 40 years on. Nat Rev Cancer. 2004 Oct;4(10):757-68. PubMed PMID: 15510157.

Yu K, Chedin F, Hsieh CL, Wilson TE, Lieber MR. R-loops at immunoglobulin class switch regions in the chromosomes of stimulated B cells. Nat Immunol. 2003 May;4(5):442-51. PubMed PMID: 12679812.

Zarrin AA, Alt FW, Chaudhuri J, Stokes N, Kaushal D, et al. An evolutionarily conserved target motif for immunoglobulin class-switch recombination. Nat Immunol. 2004 Dec;5(12):1275-81. PubMed PMID: 15531884.

Zhang B, Yin Y, Lai RC, Lim SK. Immunotherapeutic potential of extracellular vesicles. Front Immunol. 2014;5:518. PubMed PMID: 25374570; PubMed Central PMCID: PMC4205852.

zur Hausen H. Condylomata acuminata and human genital cancer. Cancer Res. 1976 Feb;36(2 pt 2):794. PubMed PMID: 175942.

zur Hausen H. Viruses in human cancers. Eur J Cancer. 1999 Dec;35(14):1878-85. PubMed PMID: 10711230.

zur Hausen H. Human papillomavirus & cervical cancer. Indian J Med Res. 2009 Sep;130(3):209. PubMed PMID: 19901427.

zur Hausen H. Similarities of papillomavirus infections with tumor promoters. Princess Takamatsu Symp. 1983;14:147-52. PubMed PMID: 6097579.

zur Hausen H. Papillomaviruses in the causation of human cancers - a brief historical account. Virology. 2009 Feb 20;384(2):260-5. PubMed PMID: 19135222.

Zwicker JI, Liebman HA, Neuberg D, Lacroix R, Bauer KA, et al. Tumor-derived tissue factor-bearing microparticles are associated with venous thromboembolic events in malignancy. Clin Cancer Res. 2009 Nov 15;15(22):6830-40. PubMed PMID: 19861441; NIHMSID: NIHMS140312; PubMed Central PMCID: PMC2783253.